TEMPERATURE CONTROL STRATEGIES FOR RADIANT FLOOR HEATING SYSTEMS

Zhi Long Zhang

A thesis in

Department of Building, Civil and Environmental Engineering

Presented in Partial Fulfilment of the Requirements

for the Degree of Master of Applied Science at

Concordia University

Montreal, Quebec, Canada

January 2001

ABSTRACT

Temperature Control Strategies for Radiant Floor Heating Systems

Zhi Long Zhang

A dynamic model of a radiant floor heating (RFH) system useful for control analysis is developed. The overall model consists of a boiler, an embedded tube floor slab and building enclosure. The overall model was described by nonlinear differential equations, which were solved using finite numerical methods.

The predicted responses from the model were compared with published experimental data. The comparisons were made covering a wide range of weather and operating conditions under several different control strategies. The model predictions compare well with the experimental data. The effective thermal capacity of the floor slab was found being an important parameter in calibrating the model results with the experimental data.

Three different control strategies for improving the temperature regulation in RFH systems are proposed. These are: a multistage on-off control, an augmented constant gain control (ACGC) and a variable gain control (VGC).

Simulation results show that the multistage control maintains zone air temperature close to the setpoint better than the existing on-off control scheme does. Likewise, ACGC gives good zone temperature control compared to the classical proportional control. A model based approach for updating the controller gains of the VGC is proposed. Both ACGC and VGC are shown to be robust to changes in weather conditions and internal heat gains. The advantage of the control strategies proposed in this thesis is that they eliminate the use of outdoor temperature sensor required in some existing control schemes. Being simple and robust, the multistage control scheme with two stages and the ACGC are good candidate controls for RFH systems.

ACKNOWLEDGMENTS

I would like to take this opportunity to express my gratitude to my supervisor, Dr. M. Zaheer-Uddin for his invaluable guidance, encouragement and suggestions during the whole course of this study.

Gratitude is also extended to Concordia University Centre for Building Studies for the use of computer facilities, and the technical stuff who provided a great deal of technical help and advice.

With respect, love and admiration, sincerely thank my parents who are always proud of me.

TABLE OF CONTENTS

LIST OF FIGURES

LIST OF TABLES

NOMENCLATURES

A	area (m^2)
ACGC	augmented constant gain control
ACH	air changes per hour
A_{en}	area of enclosure (m^2)
A_f	area of radiant floor (m^2)
A_{it}	inside area of serpentine tube (m^2)
A_w	area of window (m^2)
a_j	heat loss coefficient of boiler surface (W/K)
C	constant
C_1	hot water pump/3-way valve controller
C_2	boiler burner controller
C_b	thermal capacity of boiler (J/K)
C_p	thermal capacity of radiant floor slab (J/K)
C_{pw}	specific heat of water (J/kgK)
CRIH	convective ratio of internal heat
c	specific heat (J/kgK)
dx	thickness of element (m)
E	control error (°C)
FSC	four-stage control
F_{en-p}	radiation angle factor from room enclosure to radiant floor panel
F_{p-en}	radiation angle factor from radiant floor panel to room enclosure

G	gain of proportional controller (1/°C)
H	length of radiant floor slab (m)
h_{it}	convection heat transfer coefficient between water and tube (W/m^2K)
I_c	solar radiation intensity (W/m^2)
K	gain factor of ACGC and VGC (1/°C)
K_p	thermal conductivity of floor slab panel (W/mK)
L	depth of radiant floor slab (m)
LMTD	logarithmic-mean temperature difference (°C)
MM	mass flow modulating of hot water
MRT	mean radiant temperature (°C)
M_w	water content of serpentine tube (kg)
$\dot{m}_b$	normalised mass flow of 3-way valve bypass port
$\dot{m}_s$	normalised mass flow of 3-way valve outlet port
$\dot{m}_w$	mass flow rate of water (kg/s)
P	pitch of serpentine pipe in radiant floor slab (m)
Q_c	convection heat transfer (W)
Q_r	radiation heat transfer (W)
Q_{sol}	solar radiation impinging on enclosure exterior surface (W)
q_c	convection heat transfer (W)
q_{ig}	internal heat gain (W)
q_{inf}	infiltration heat loss (W)
q_r	radiation heat transfer (W)

q_{sol}	solar radiation passing through window (W)
RFH	radiant floor heating
SF	shading factor
SPC	single-parameter control
TM	temperature modulating of hot water
TPC	two-parameter control
TR	throttling range
TSC	two-stage control
T_e	temperature of boiler room (°C)
T_{en}	temperature of interior surface of enclosure (°C)
T_o	temperature of outdoor air (°C)
T_{ex}	temperature of exterior surface of enclosure (°C)
T_{rt}	temperature of return water (°C)
T_{set}	temperature of setpoint (°C)
T_{sl}	temperature of radiant slab surface (°C)
T_{sp}	temperature of supply water (°C)
T_{s2}	middle layer temperature of radiant slab (°C)
T_{s3}	bottom layer temperature of radiant slab (°C)
T_z	temperature of zone air (°C)
t	time (s)
U	normalised energy input
U_b	normalized energy input of boiler
U_{bmax}	maximum energy input of boiler (W)

$U_{ceiling}$	U-value of ceiling (W/m^2K)
U_w	normalized mass flow rate of hot water
U_{wall}	U-value of wall (W/m^2K)
U_{window}	U-value of window (W/m^2K)
U_{wmax}	maximum mass flow rate of hot water (kg/s)
U(n)	normalised input of a system at time n
V	volume (m^3)
VGC	variable gain control
W	width of radiant floor slab (m)
α	admittance of window glass
ε	steady state control error (^oC)
η_{com}	combustion efficiency of burner
ρ	mass density of zone air (kg/m^3)

CHAPTER 1

INTRODUCTION AND LITERATURE REVIEW

1. 1. Introduction

Radiant heating is one of the oldest techniques used by man for warming up a living space. Through its use man could separate fuel burning and combustion products away from the living space to keep it clean and safe. The radiant panel, embedded in the floor and/or wall, was made by heavy materials so that it could continuously release heat to the heated space after the fire ran out. This therefore not only made the operation more convenient and easier to handle but also provided much needed comfort. Today, water as the heat transport medium has taken the place of direct fire inside the radiant panel in most applications. Beside of heating, radiant cooling panel is also in practical use today.

Radiant floor heating (RFH) system offers various advantages in space conditioning. These include almost no noise, low draft, no requirement for cleaning, free use of space, uniform temperature distribution, energy saving potential, favourable tie in capabilities with low temperature and low intensity energy sources. More than half the thermal energy emitted from a RFH system is in the form of radiant heat. The convective heat from a RFH system is delivered directly to the occupied zone at floor level, where the occupants are. The radiant heat directly influences the heat exchange with the occupants and surrounding surfaces such as walls and ceiling. In this way a uniform

thermal environment is established. As such lower zone air temperature will be required to keep occupants in thermal comfort condition thereby reducing energy consumption.

Radiant panel heating systems also have the potential to reduce air infiltration consequently reducing the energy consumption. A 12.5% reduction in the natural air infiltration compared to the forced-air heating system was reported in the study conducted by Yost, Barbour and Watson (1995) [34]. They also evaluated a ceiling radiant panel using thermal comfort parameters and stated, "the radiant heating system demonstrated significantly better energy performance than the either the heat pump or base-board system".

Watson, Chanpmam and DeGreef (1998) [33] have studied seven different heating systems. The data from pre- and post-retrofit of 100 units, being monitored for two to four years, had been analysed. The results show that the use of the fast-acting radiant heating system saved energy up to 14.6%.

Even through the advantages of RFH system over the conventional heating systems are well recognized, the one area which requires further studies concerns the development of improved control strategies for operating the RFH systems as will be demonstrated in literature reviews presented in this chapter. Therefore, this study focuses on modelling and control of RFH systems. A dynamic model of RFH system will be developed. The predictions from the developed model will be compared with the

published experimental results. The validated model will be used to explore improved control strategies for operating the RFH system. The thesis is organized as follows:

1) In Chapter 2 an analytical model of RFH system is developed.
2) Results from the validation of the model are presented in Chapter 3.
3) In Chapter 4, in particular a multi-stage control method and its applications to RFH systems are discussed.
4) An augmented constant gain and a variable gain control strategy are developed in Chapter 5. Several simulation results are presented to show the advantages of the developed control strategies compared to the traditional control techniques.

1. 2. Literature Review

The literature survey is organized in three sub-sections:

(i) Studies dealing with modelling of RFH systems,

(ii) RFH system control, and

(iii) Experimental studies.

1. 2. 1. A Review of RFH System Models

The steady state analysis techniques have been widely used specially for the design and energy analysis of RFH systems. Banhidi's book (1991) [5] describes nonlinear radiant and convective heat transfer processes taking place in a radiantly heated

enclosure. The equations were linearized by using experimental corrections. Kilkis and Coley (1995) [19] developed a simple model for determining radiant slab surface temperature and heat flux. Kilkis and Spapci (1995) [18] also developed a computer program for the radiant panel design and analysis purposes. A practical method for the design of radiant panel systems can be found in ASHRAE HVAC Systems and Equipment Handbook (1992) [2].

Hogan and Blackwell (1986) [16] developed a steady state model using finite element method to evaluate the performance of a hot water concrete floor heating panel. They found that the downward and edgewise heat losses computed by using the ASHRAE method were somewhat overestimated.

Zhang and Pate (1986) [37] employed a finite-difference algorithm to simulate the heat diffusion in a ceiling panel. They predicted the ceiling surface temperature by simulating steady state and transient heat transfer processes.

The temperature of electric element is a key factor in the design of electric heating radiant panel. Ritter and Kilkis (1998) [27] introduced a steady-state fin model to size an electric radiant panel. They have introduced an adjustment factor to model a two-dimensional fin for predicting the heating element skin temperature.

Thermal comfort issues of RFH systems have received increased attention by more and more researchers. Since the mean radiant temperature (MRT) of a radiant

system has a governing impact on thermal comfort, The MRT should be considered during the design process. The paper by Kalisperis, el. al. (1990) [17] presents a method for designing radiant panel heating system using MRT as basis for thermal comfort decision making. To evaluate the radiant heating system performance in terms of thermal comfort, Ling and Deffenbangh (1990) [22] developed a computer model for determining the average predicted percentage dissatisfied (APPD) index useful for assessing low-temperature radiant heating systems.

Studies on radiant panel system with solar gains are available in the literature. For example, Athienitis (1994) [3] presented a transient approach to solve an explicit nonlinear-difference network model and predict the performance of a floor radiant heating system with high solar gain.

In order to accurately predict the short term control dynamics, Savery and Lee (1996) [29] described the thermostat by a digital, nonlinear model. A fourth-order state-variable digital model of a residence heated with electric unit heaters was developed. They used a five-parameter building model which included the capacitance of the structure, capacitance of the contents of the house, conductance associated with the structure. A three-parameter nonlinear thermostat model included the value of the proportional gain, switching differential and time constant. And a lumped capacity first-order model described the electric heater. The results of the simulation show a good match with the measured data.

Brickman and Moujaes (1996) [7] developed a detailed model. The radiation exchange among the interior walls and internal structure was taken into account. Instead of using conduction heat transfer to model the heat exchange in the air gaps, the effects of free convection occurring in the trapped air in the internal wall structure were modeled. They also added free convection on exterior surfaces and forced convection effects from wind. Comparisons were made with the recorded temperature measurements, which resulted in a prediction accuracy generally within the error tolerances of the experimental measurements of $\pm 1^{\circ}C$ throughout the room's structural elements and in the interior air over the course of a day.

Dunne and el. (1996) [12] developed algorithms for modelling the interreflected solar heat gain from neighbouring structures and implemented the algorithms in a building energy simulation program. The algorithms account for the contribution from unobstructed and interreflected solar radiation in the solar heat gain through opaque and transparent surfaces. The algorithms use a freeware ray-tracing program which models specularly and diffusely reflecting surfaces under varying sky conditions. It was modified to account for irradiance values including the absorbed solar radiation in transparent surfaces. They found that the solar gain from specularly reflecting surfaces could be ten times that from diffusely reflecting surroundings.

Recently a number of researchers have involved thermal comfort parameters into their models. Chapman (1997) [9] had studied a case by employing building comfort analysis program (BCAP) to analyse the thermal comfort distribution of a radiant heating

system. By comparing the energy consumption of radiant system with conventional forced-air system, Strand and Pedersen (1997) [32] showed that the radiant system is more efficient while offering the same thermal comfort conditions.

Chapman and Zhang (1996) [10] developed a three-dimensional mathematical model to compute heat transfer within a radiantly heated or cooled room. To analyse the effect of non-uniform wall temperatures and properties, they modelled the room by a discrete ordinate radiation model, which calculates the mass-averaged room air temperature and the wall surface temperature distributions.

Freestone and Worek (1996) [13] simulated a three-story building in which a ceiling heating/cooling radiant panel was installed. They found that by removing the insulation from the top of the panel and placing a partition in the ceiling plenum to concentrate the heat in the perimeter area can either reduce the energy consumption or improve the mean radiant temperature distribution. Simmonds' (1996) [31] study also shows the same result from a radiant panel system that was installed close the windows.

The impact of reflectivity of wall in a radiant panel heating system was studied by Saunders and Andrews (1987) [28]. By means of a transient heat transfer model, they studied the radiative and convective heat exchange of wall and radiant panel. Their results suggested that reflective walls could reduce the heat loss to the weather by reducing the wall temperature. And the walls also radiate higher equivalent blackbody temperature by reflecting the heating panel radiation.

Since room air distribution is not uniform in most cases, the thermal comfort parameters measured by a sensor, which is often located outside the occupied zone, are different from those in the occupied zone. It is necessary to identify a suitable position for the sensor and to find the correlation of the comfort parameters between the sensor zone and the occupied zone. Chen and el. (1996) [11] used a flow model, a conjugate heat transfer model and a radiant model, which were solved simultaneously in a computational fluid dynamics (CFD) program. They proposed a correlation for finding the most suitable position for locating the sensor.

1. 2. 2. Radiant Heating System Control

The conventional on-off control is still the dominant mode of control in the radiant floor heating systems. However, the heavy structure with large thermal storage can delay the control response causing the controlled temperature with relatively large derivation from the setpoint. A number of alternative control strategies have been introduced in last decade.

MacCluer (1989) [25] studied outdoor temperature reset control by considering the heat loss through building enclosure in steady state. The heat demand of the building was described as a linear function proportional to outdoor temperature. The constant of proportionality relating the rise in water temperature to the drop in outdoor temperature (called the reset slope) was used in the control equation. When the outdoor temperature

decreases the controller operates the system by either increasing the supply water temperature or by increasing the water flow rate.

The indoor temperature is affected not only by outdoor temperature but also by internal heat gain, solar radiation and so on. To account for these effects MacCluer (1991) [23] proposed outdoor reset control with an indoor feedback as offset.

Gibbs (1994) [14] built up a model to simulate the control strategies of a multi-zone RFH system. The simulations used zone air temperature with a setpoint of 20°C. The outdoor temperature was modelled as a sinusoid function with a 24-hour period and by a step function. Three control strategies: (1) pulse-width-modulated zone valves with a constant-temperature boiler, (2) outdoor reset with indoor temperature feedback, and (3) outdoor reset plus pulse-width-modulated zone valves were studied.

The simulation of first control strategy assumed that the supply water temperature of 50°C remained relatively constant whether one or several zone valves were open. The room thermostats had a 1.67°C proportional band and pulse-width-modulated the zone valves four times per hour. In order for the room air temperature to reach the setpoint (20°C), the valve was on for 7.5 minutes and off for 7.5 minutes, while at 20.5°C the valve was on for 3 minutes and off for12 minutes.

In the second simulation the supply water for the system was regulated through a mixing valve and outdoor reset control. The outdoor reset control in this model is only a

proportional control but it has indoor temperature feedback. The indoor feedback was found to have a limited effect on the supply water temperature. The reset ratio of the model was set constant at 0.66.

In the third simulation results presented by Gibbs (1994) [14] the RFH system was modelled by combining both pulse-pulse-width-modulated zone valves and outdoor temperature reset with indoor temperature feedback. The supply water temperature for this case was regulated through a mixing valve and outdoor reset control, and water flow into each zone was turned on and off by pulse-width-modulated zone valve. The results of the simulations indicate that the strategy of outdoor reset plus pulse-width-modulated zone valve offers the most advantages.

Zaheer-Uddin el. al. (1994) [35] developed a nonlinear model of a radiant floor system. The mathematical model was based on the energy balance method. Model equations for the boiler, floor slab, conditioned space and outdoor environment were solved simultaneously using finite difference techniques.

To improve the steady state heat transfer approach used in his earlier studies, MacCluer (1990) [24] set up a transient model in which the flow rate was kept constant while the temperature of the water sent to the floor slab was proportional to outdoor temperature. In the model the transfer function was written in analytical form and was solved in frequency domain. The reset slope was no longer a constant but a function of the outdoor temperature and the room transfer function.

Athienitis and Shou (1991) [4] utilized a numerical model using detailed room transfer functions for the operative temperature and simple Laplace transfer functions for the heating and control system components. It was shown that the response to setpoint changes of the radiant heating system using an operative temperature sensor indicated significant potential for faster control than using an air temperature sensor.

1. 2. 3 Experimental Studies

Zhang and Pate (1986) [36] measured the performance of a radiant panel ceiling heating system. The ceiling panel was built in the concrete slab in which hot water copper tubes were embedded. The supply-return tubes were lined parallel and counter flow to each other. Their results show that the ceiling temperature distribution was uniform. The interesting result they found that the room air temperature did not lag the wall and floor temperature and the transient response of the radiant system was sensitive on hot water supply temperature but not as sensitive to the hot water flow rate.

Space air temperature on-off control may be the simplest method available and is widely used in HVAC systems. A heavy building structure causes thermal lag or delay, which will cause large fluctuations in the floor temperature. An experimental test facility, in which the rooms were heated by a RFH system, was used by Cho and Zaheer-Uddin (1997) [8] to study the effect of different control strategies. The measurements included

three different cases, 1) room air temperature on-off control, 2) floor slab temperature on-off control, and 3) the combination of the room air and floor slab temperature on-off control. The test results show that the conventional room air on-off control can cause larger temperature swings in both room air and slab temperature compared with slab temperature control. The slab on-off control alone, on other hand, may not be suitable in rooms with large internal heat gain. The combination of the room air and floor slab temperature on-off was shown to be effective control strategy.

Olesen (1994) [26] has tested a wall heating panel system and a floor heating panel system. The results show both floor and wall panel system were able to maintain a comfortable thermal environment under dynamic conditions including solar radiation, internal heat gain and temperature setback, etc. The systems also consume similar level of energy.

The temperature distribution in the heated space was measured by Hanibuchi and Hokoi (1998) [15]. Their data show that the floor heating produces an approximately uniform air temperature distribution and the convective heat exchange contributes about half of the heat output.

Leigh (1991) [20] set up an experimental system to compare the temperature and heat flux control using outdoor air temperature reset. The results show that the proportional flux modulation resulted in faster response to certain thermal transients than does the outdoor reset control with indoor temperature offset.

Scheatzle (1996) [30] conducted tests in a heavy structure single-family house with a radiant/convective system for both heating and cooling. The test had been designed to provide superior comfort by using the so called comfortstat which takes into account six variables of human comfort (activity level, clo value, ambient air temperature, mean radiant temperature, air velocity and humidity), and a programmable controller. His findings show that a superior comfort can be achieved by employing the operative sensors and the programmable controller. However, the hardware and installation costs were high for residential applications.

Lindstrom, Fisher and Pedersen (1998) [21] have examined the impact of surface characteristics on radiant panel heat output. They recommended the radiant slab emissivities of 0.90 to 0.95 could be used for engineering calculation of radiative heat transfer. The fraction of total panel output convected from radiant floor panel surface is as high as 30%.

1. 3. Summary

From the literature review the following issues were identified.

1) A great majority radiant heating system models are of the steady state type. As such they are intended for the design rather than operation and control studies.
2) Except for reference [35] the available models mainly focussed on the radiant heat exchange and comfort issues at the zone level. Therefore the control

strategies proposed in the literature ignore the system dynamics such as those due to the boiler operation.

3) The model presented in reference [35] considers the dynamic effects of the boiler and the radiant floor together with a zone load model, which ignore the thermal inertia effects of the enclosure. Furthermore, the model in [35] requires solutions of 30 nodal equations to predict the room temperature. Also, the optimal control solution presented in [35] is too complex for practical implementation using simple control hardware.

4) The control strategies studied in the literature are proportional control with outdoor air reset. This strategy requires a good correlation between zone load, outdoor temperature and supply water temperature. In the absence of accurate knowledge of such a function, either over correction or poor control could result.

1. 4. Objectives of the Thesis

This thesis addresses some of the limitations noted above concerning modelling and control of RFH systems. To this end, the major objectives of this thesis are:

(i) To develop a relatively accurate and computationally efficient dynamic model of radiant floor heating system useful for operation and control studies.

(ii) Validate and calibrate the developed model using experimental field data.

(iii) Develop simple and effective control strategies for efficient operation of RFH systems.

(iv) Carry out simulation runs to study and evaluate the performance of different control strategies.

Many researchers have developed various kinds of models for different purposes as described previously. From single zone to multizone, most models focus on the indoor temperature performance in accordance with weather disturbance. In practice, a system is running under the combination of the disturbances, from heating source to internal heat gain. Such that it is necessary to develop a new model, which includes a boiler, heat emission device, control device and zone. In order to verify the stability of the control system performance, the weather disturbances, internal heat gain and heat source must be taken into account simultaneously.

CHAPTER 2

DYNAMIC MODEL OF

RADIANT FLOOR HEATING (RFH) SYSTEM

2. 1. Introduction

In this chapter a dynamic model of RFH system useful for control and operation studies will be developed. First the physical system will be described. Then dynamic models of each component will be developed and integrated to simulate the performance of a RFH system.

The model given in reference [35] will be used as a basis to develop a simpler model useful for simulating different control strategies. This is needed because model in reference [35] requests thirty-two nonlinear differential equations to simulate the dynamic performance of the RFH system. Furthermore, it needs estimation of several parameters to validate its predictions. For these reasons, it is necessary to develop a simple model, which can be calibrated easily using experimental results.

2. 2. Radiant Floor Heating (RFH) System

A typical single zone RFH system, shown in Figure 2.2.1, consists of a radiant floor slab embedded with serpentine tube in which hot water is circulated using a circulating pump and distribution piping. The major components of RFH system include:

a hot water boiler, circulating pump, piping network, an embedded pipe radiant floor in an environment zone and a control system. In response to the demand for heat from the zone thermostat, the pump is operated by the controller C_1. The controller C_2, simultaneously, controls the burner of the boiler in an on-off mode such that the supply water temperature is maintained within a chosen high/low limit, for safety, the burner is shut off when the circulating pump is off.

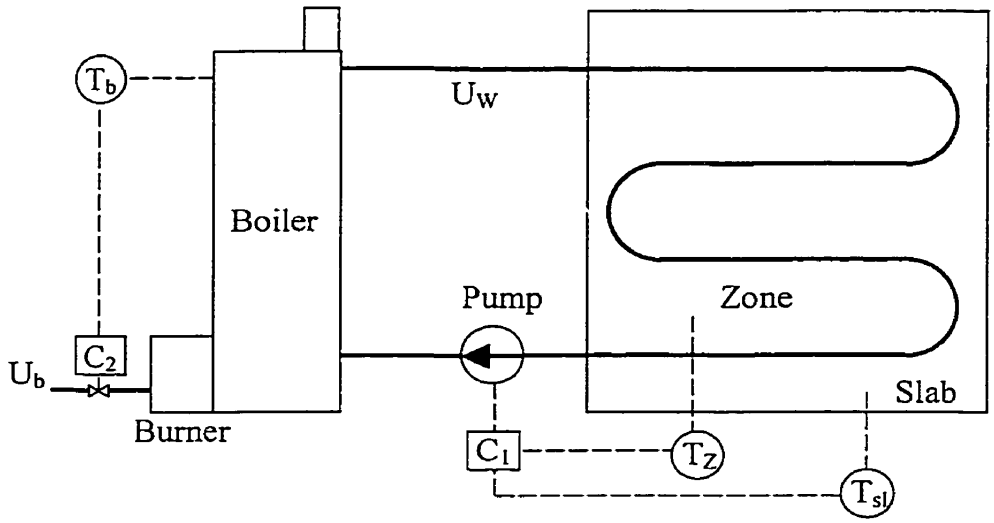

Figure 2.2.1 Schematic diagram of a floor heating system

Since more than half of the heat released from floor slab is in radiation, the nonlinear nature of heat fluxes have to be taken into account. A dynamic model of the RFH system should incorporate all aspects of heat transfer mechanisms, conduction, convection, radiation and thermal storage, affecting the temperature response of the system. A dynamic model will be developed by applying the energy balance principle on each of the components representing a gas-burning boiler, a concrete floor slab with

serpentine tube and a room with thermal capacity. Each component will be modelled individually based on its own physical arrangement by applying energy balance technique. The resulting time dependent differential equations will be solved using finite numerical techniques.

2. 3. Radiant Floor Model

A hydronic radiant floor typically consists of a serpentine pipe embedded in a concrete slab shown in Figure 2.3.1. Hot water inside of the serpentine tube passes heat to the slab from which the heat is released to the space by radiation and convection. There is an insulation under the slab to reduce the heat loss to the ground.

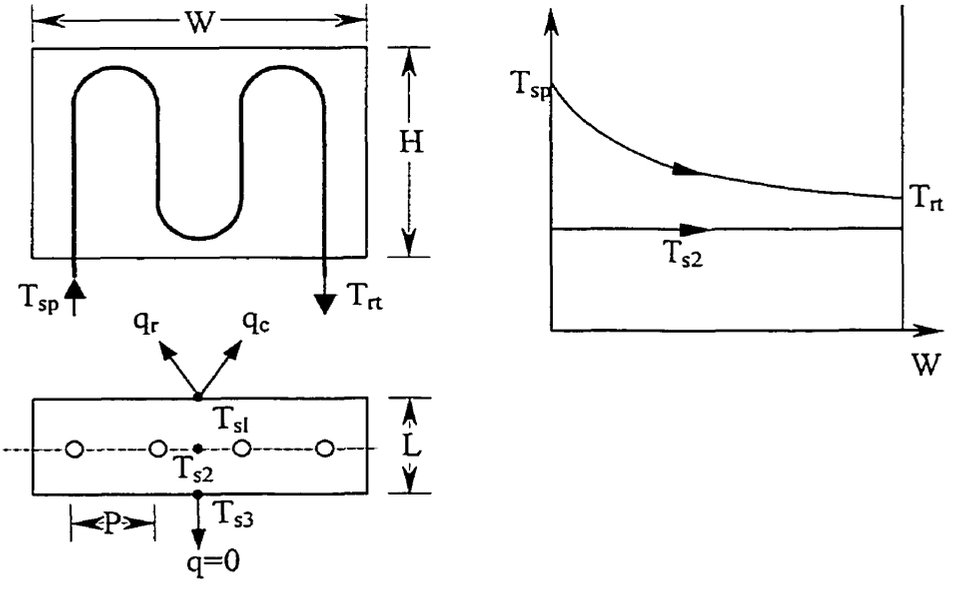

Figure 2.3.1 Schematic diagram of floor slab with nodal arrangement and assumed temperature distribution

A slab is considered with dimensions W×H and thickness L as shown in Figure 2.3.1. The tube pitch is P. The temperature distribution of the slab surface is not uniform since hot water inside of serpentine pipe gives up heat thereby its temperature and consequently the slab surface temperature decreases in the water flow direction. Also for thermal comfort reason the floor surface temperature of most RFH systems has to be limited so that a low temperature drop of hot water is widely used in practice. The test results show that for hot water temperature drops of about 7°C the resulting floor surface temperature difference is less than 2°C. Together with these considerations the following assumptions were made to develop a simple model of radiant floor.

(1) The temperature distribution inside slab is uniform in horizontal direction that no heat transfer occurs horizontally.
(2) The slab properties are homogenous.
(3) The heat transfer from hot water inside of the serpentine pipe to the floor slab is described by a logarithmic-mean-temperature-difference (LMTD).
(4) No heat loss through the insulation to the ground.
(5) No heat loss through the distribution pipe.

The heat transfer process then can be simply considered as one-dimensional problem. To develop energy balance equations describing the heat transfer processes between the water circulating in the pipe and the slab surface, the slab was described by three nodes and the temperatures of the nodes are presented by T_{s1}, T_{s2} and T_{s3}

respectively as shown in Figure 2.3.1. The hot water gives up heat at node 2 (T_{s2}) and the slab releases the heat to the space being heated by radiation and convection at node 1 (T_{s1}). There is no heat loss through the insulation (node 3 at T_{s3}). However node 3 does affect the temperature distribution of the slab via its thermal storage.

Since the floor slab is interacting with boiler hot water on one side and enclosure temperature on the other side, the coupling effects are modelled using supply water temperature T_{sp}, which is associated with boiler energy output from boiler model; room air temperature, T_z, and enclosure interior surface temperature, T_{en} from room model. The return water temperature, T_{rt}, and slab surface temperature, T_{s1}, are the outputs which will be determined by the radiant floor model. The heat transfer process is described by the following nodal equations.

$$C_p \frac{dT_{s1}}{dt} = \frac{K_p A_f}{dx}(T_{s2} - T_{s1}) - q_r - q_c \qquad (2.3.1)$$

$$C_p \frac{dT_{s2}}{dt} = -\frac{K_p A_f}{dx}(T_{s2} - T_{s3}) - \frac{K_p A_f}{dx}(T_{s2} - T_{s1}) + \dot{m}_w C_{pw}(T_{sp} - T_{rt}) \qquad (2.3.2)$$

$$C_p \frac{dT_{s3}}{dt} = \frac{K_p A_f}{dx}(T_{s2} - T_{s3}) \qquad (2.3.3)$$

Where

$$q_r = 5 \times 10^{-8} F_{p-en} A_f \{[T_{s1} + 273]^4 - [T_{en} + 273]^4\} \qquad (2.3.4)$$

$$q_c = 213 A_f (T_{s1} - T_z)^{1.31} \qquad (2.3.5)$$

In equation 2.3.4 $F_{p\text{-}en}$ represents radiation angle factor from floor slab panel to structural enclosures that it equals to 1.0 for flat panel. Equation for T_{rt} and T_{en} are given as follows:

$$\frac{dT_{rt}}{dt} = \frac{h_{it}A_{it}}{M_w C_{pw}}(LMTD) + \frac{\dot{m}_w C_{pw}}{M_w C_{pw}}(T_{sp} - T_{rt}) \tag{2.3.6}$$

and LMTD can be obtained from figure 2.3.1

$$LMTD = \frac{(T_{sp} - T_{s2}) - (T_{rt} - T_{s2})}{\ln\left(\frac{T_{sp} - T_{s2}}{T_{rt} - T_{s2}}\right)} \tag{2.3.7}$$

The enclosure surface temperature T_{en} was computed by solving equations for the room model.

2. 4. Room Model

The warmer floor slab surface of a RFH system exchanges heat to the colder enclosure surfaces by radiation. The zone air receives heat from the slab and gives up to the colder surfaces of enclosure by convection. The enclosure heat gains should compensate the heat lost to the weather. The temperature distribution of heated enclosure is impacted by a numbers of factors listed following:

1. Mean floor slab surface temperature, T_{sl}.
2. Internal heat generation, q_{ig}.
3. Infiltration, q_{inf}.
4. Outdoor air temperature, T_o.
5. Solar radiation, Q_{sol} impinging on the exterior enclosure surfaces, and q_{sol} through window impinging on the interior enclosure surfaces.

All of these are time dependent variables and are considered as discretized inputs in the model equations.

In the room model the air temperature, T_z, and enclosure interior surface temperature, T_{en}, is taken as uniform throughout all of the space. This means that those temperatures depend upon time rather than location. The vector of temperature change rate with time, $\{\dot{T}\}$, of the elements can then be expressed as

$$\{\dot{T}\} = [C]^{-1}(\{Q\} - [K]\{T\}) \qquad (2.4.1)$$

Where the vector [T] represents inside, middle and outside nodal temperature respectively. The [K] represents conductance of the room and the [C] describes the effective thermal capacity of the room. Because there is no heat being added or removed inside of enclosure nodes, all the values of the heat vector {Q} in the equation, if more than one element is used, are zero except those due to surface boundary conditions.

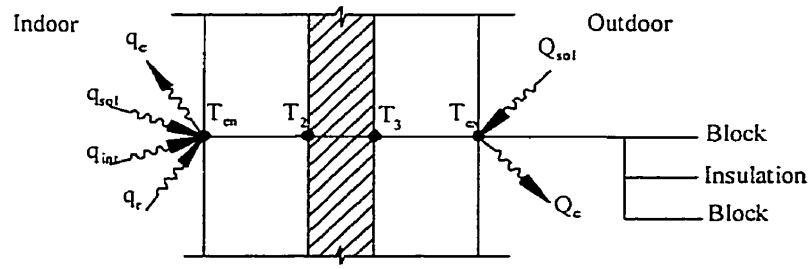

Figure 2.4.1 Typical wall section and heat fluxes

As shown in figure 2.4.1, at the interior surface of the enclosure the heat fluxes include floor slab radiation, internal heat gains, solar radiation through the window and exchange with zone air. The infiltration air mixed with the indoor air interacts convectively with the interior surface.

The radiation heat flux q_r is modelled as [2]

$$q_r=5\times10^{-8} F_{en-p} A_{en} [(T_{sl}+273)^4-(T_{en}+273)^4] \quad (2.4.2)$$

The F_{en-p} is radiation angle factor from enclosures to radiant panel. The equation 2.4.2 and 2.2.4 describe the same radiant heat flux. The convective heat flux, q_c, to the room air, at temperature T_z, is given by ASHRAE Handbook Fundamentals [1]

$$q_c=1.31A_{en} (T_z-T_{en})^{1.33} \quad (2.4.3)$$

The infiltration air mixes with zone air directly. If ACH is the rate of air change per hour, then q_{inf} is calculated from:

$$q_{inf} = V\rho\, c(T_o-T_z)\, ACH/3600 \quad (2.4.4)$$

Where V is the volume of the room, ρ is mass density, c is specific heat of air and T_o is the outdoor air temperature.

Solar radiation in the model has two components, the one representing solar gains through glass of window casting on the interior surface of the enclosure, and the another in the form of solar radiation impinging on the exterior surfaces of the enclosure. If I_c is solar radiation intensity, α the admittance of the glass and shading factor (SF), then q_{sol}, entering the room through the window in A_w of area, can be calculated from:

$$q_{sol} = A_w SF\alpha I_c \quad (2.4.5)$$

The thermal capacity of room air is small so that it can be ignored. The energy balance equation on room air can be described by following steady state equation:

$$2.13A_f(T_{sl}-T_z)^{1.31}+1.31A_{en}(T_{en}-T_z)^{1.33}+(CRIH)q_{ig}-q_{inf}=0 \quad (2.4.6)$$

Where (CRIH) refers convective ratio of internal heat.

There are two heat fluxes adding on the exterior surface of the enclosure, the Q_{sol} and Q_c (convection). In winter conditions the velocity of outdoor air is considered high and the convection heat exchange can be recognized as a linear function of the temperature difference. ASHRAE Handbook Fundamentals [1] recommends 34w/Km^2 of the exterior surface convective coefficient in winter. Therefore Q_{sol} and Q_c were modelled as follows:

$$Q_{sol} = A_{en}SFI_c \quad (2.4.7)$$

$$Q_c = 34A_{en}(T_o-T_{ex}) \quad (2.4.8)$$

There T_{ex} is exterior surface temperature.

2. 5. Boiler Model

In the reference [35] the energy balance equation of the boiler model was described as

$$C_b\frac{dT_{sp}}{dt} = \eta_{com}U_bU_{b\max} - U_wU_{w\max}C_w(T_{sp}-T_{rt}) - a_j(T_{sp}-T_e) \quad (2.5.1)$$

Where C_b is thermal capacity of boiler, C_w is thermal capacity rate of water, a_j is the rate of the heat loss from boiler jacket to the environment (the boiler room) and T_e is the temperature of the boiler room.

The water mass flow rate U_w is normalized with respect to maximum flux rate so that U_w in equation 2.5.1 varies between 0 and 1. The circulating pump can be controlled by a feedback signal from room air temperature or floor slab surface temperature or both of them.

The burner as energy input device works in an on-off mode using T_{sp} as feedback signal. The energy input, $U_b U_{bamx}$ represents the maximum burner capacity when $U_b = 1$. It is too complex to describe the combustion process mathematically since the flame temperature and flow gas temperature are affected by too many factors. However an empirical model is used to describe the combustion efficiency of the boiler. The combustion efficiency is given by a polynomial such as:

$$\eta_{com} = a_1 + a_2\left(\frac{T_{sp}}{T_{sp\,\max}}\right) + a_3\left(\frac{T_{sp}}{T_{sp\,\max}}\right)^2 + a_4\left(\frac{T_{sp}}{T_{sp\,\max}}\right)^3 + \bullet\bullet\bullet \qquad (2.5.2)$$

Where the coefficients can be obtained from experimental data. In this study we have assumed $a_1 = 1$ and $a_2 = -0.12$ which corresponds to a rated efficiency of 88% for the boiler at maximum supply water temperature.

2. 6. Overall RFH System Model

The equations describing the radiant floor slab, the room and the boiler taken together constitute the overall model equations describing the dynamic performance of the RFH system. The model consists of eight differential equations, which were solved using finite numerical methods.

As noted in section 2.1, the developed model is simpler (has less number of equations than those in reference [35]) and therefore requires less computational time to solve the equations. In order to compare the accuracy of predictions from the present model simulation runs were made and results were compared with those from the model given in reference [35] and as well as published experimental data from a test utility [8]. These comparisons are depicted in Figure 2.6.1 and 2.6.2. It is noted that reference [35] uses 14 nodes to describe the temperature distribution whereas the present model uses logarithmic-mean temperature difference (LMTD), which is considered uniform over the width of the slab. The predictions from the present model compare well with the measured data as shown in Figure 2.6.1 and 2.6.2. Therefore, we conclude that the present model is simpler to use and can be used to explore various operating strategies. Before developing new control strategies the predictions from the model will be compared with measured data under several different operating conditions. These comparisons will be used to calibrate the model parameters if necessary and to validate the accuracy of predictions.

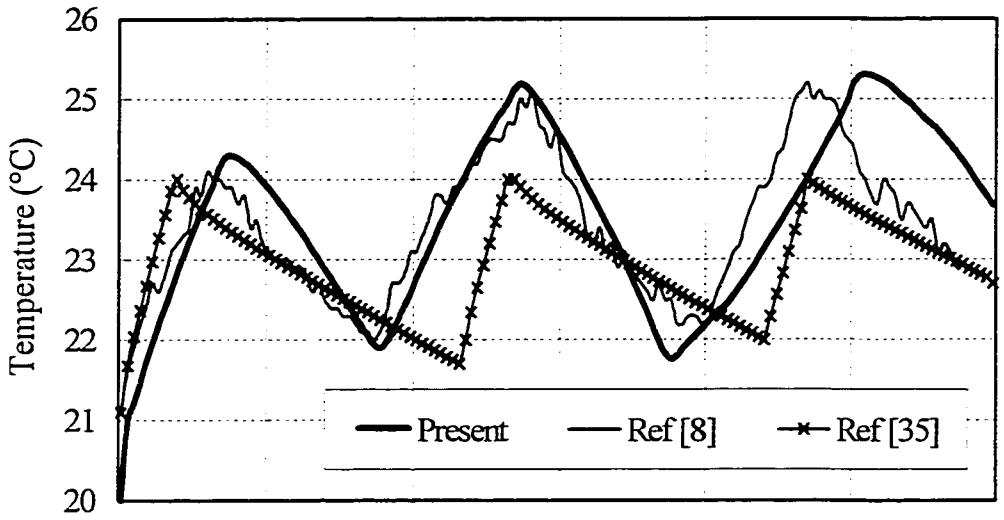

Figure 2.6.1 Comparison of predicted room temperatures with published data

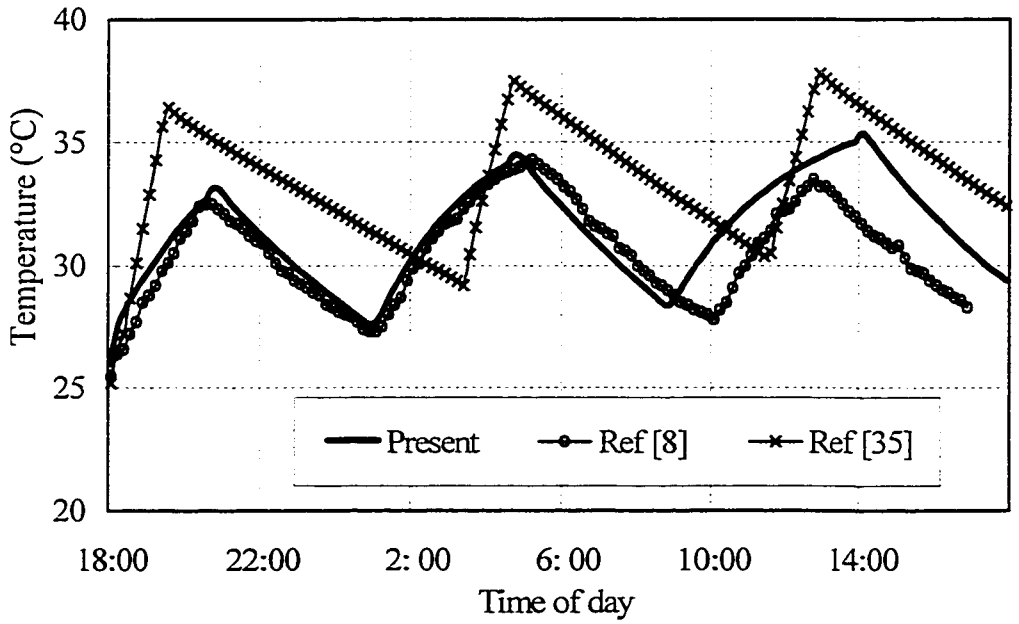

Figure 2.6.2 Comparison of predicted slab temperatures with published data

CHAPTER 3

MODEL VALIDATION

3. 1. Introduction

Before developing control systems for the operation of RFH system, it is important to verify the model predictions by comparing them with experimental results. To this end, published experimental results [8] were used. It is noted here that the specifications of the test facility, design and operating parameters as well the weather data were made available for the purpose of making the comparisons as meaningful and accurate as possible. This chapter presents results of such comparisons and shows the sources of agreements and deficiencies. A brief description of the test facility [8] is given here so that the discussions on the comparison between the model predictions and experimental data [8] are easy to understand.

3. 2. The Test Facility [8]

The RFH system test facility consisting of two 3×4.4×3.8m rooms identical in construction was built in Teajon, South Korea, latitude 37.5° north. It was designed to enable simultaneous comparison of two different control strategies. The floor plan, cross sectional details of wall, radiant floor are depicted in Figure 3.2.1 and Figure 3.2.2 respectively.

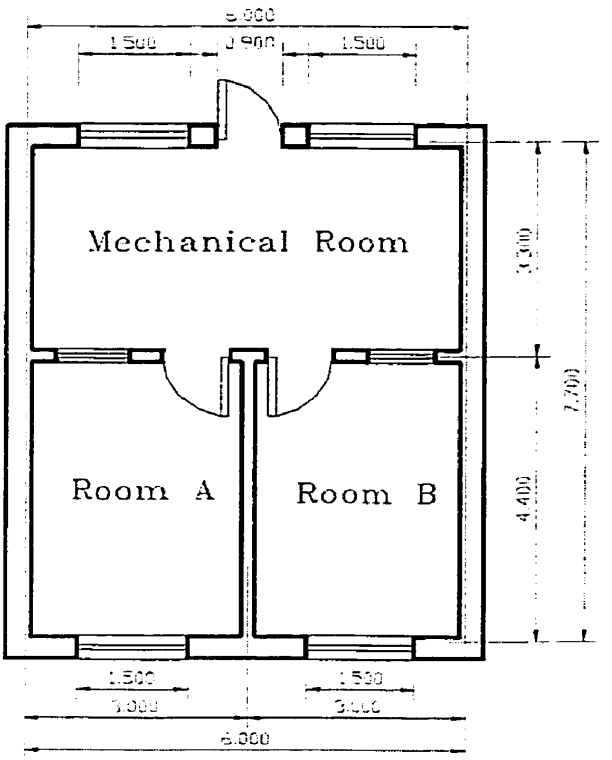

Figure 3.2.1 Arrangement of the test rooms [8]

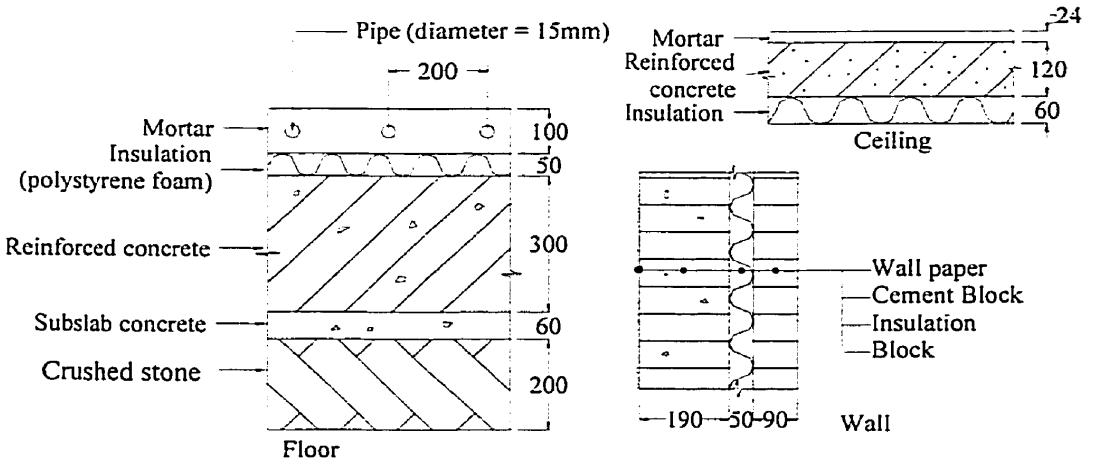

Figure 3.2.2 Cross-sectional details of the floor slab, walls and ceiling [8]

The floor slab, 3m×4.4m in area, consists of stone and concrete embedded with 15mm diameter copper pipes on 200mm centres. A 50mm polystyrene foam layer was set under the slab to reduce the heat loss (Figure 3.2.2). The construction details of the walls and ceiling are also shown in Figure 3.2.2. The hot water heating system consisting of a 6,500kcal/h (7,500W) gas-fired boiler with its piping network and circulating pumps is depicted in Figure 3.2.3. An electrically heated storage tank (with a capacity of 5kW and 400L in volume) was installed in the circuit to supply relatively constant temperature of hot water to the floor slab during the experiments.

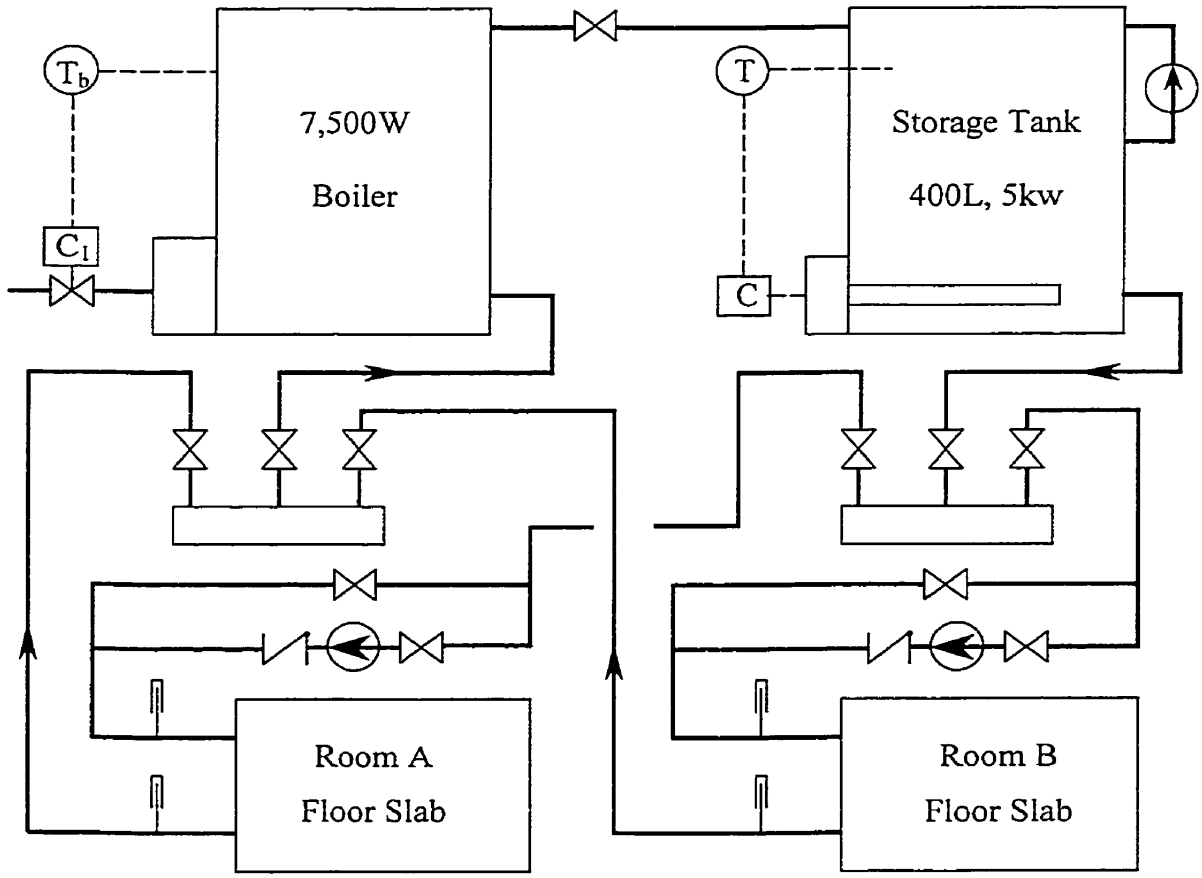

Figure 3.2.3 Schematic diagram of the hot water heating system [8]

During the tests the windows of the test rooms were covered with aluminium foil to eliminate the effect of direct solar gains through windows. Furthermore, the tests were conducted with no internal heat sources.

The measured data consisted of room air, outdoor air and floor slab surface temperatures. The temperature of supply and return water to and from the floor slab and the mass flow rate of hot water sets of such test data conducted on several days during the heating season were made available to us for the purpose of validating the model developed in this thesis.

The design parameters used in the simulations correspond to the specifications of the test facility (Figures 3.2.1 to 3.2.3). These are summarised in the following Table 3.2.1 to 3.2.3.

Table 3.2.1 Room data of the test facility [8]

Item	**Symbol**	**Magnitude and Units**
U-value of the wall	U_{wall}	$0.66 W/Km^2$
U-value of the ceiling	$U_{ceiling}$	$0.56 W/Km^2$
U-value of the windows	U_{window}	$3.60 W/Km^2$
Zone thermal capacity	C_z	$4.20 \times 10^6 J/K$ (calibrated)

Table 3.2.2 Radiant floor slab data of the test facility [8]

Item	Symbol	Magnitude and Units
Floor slab conductance	U_p	6.25W/Km^2
Inside area of serpentine tube	A_{it}	12.36m^2
Serpentine tube water content	M_w	7.55kg
Floor slab area	A_p	13.20m^2
Floor slab thermal capacity	C_p	1.90×10^{6}J/K (calibrated)
Convection heat transfer coefficient inside tube	h_{it}	140.20W/K (calibrated)

Table 3.2.3 Boiler data of the test facility [8]

Item	Symbol	Magnitude and dimension
Boiler capacity	U_{bmax}	7500W
Boiler thermal capacity	C_b	4.24×10^{4}J/K (calibrated)
Maximum water temperature	T_{bmax}	62°C
Boiler jacket conductance	a_j	5.06W/K (assumed)
Boiler room temperature	T_e	20°C (assumed)
Pump capacity	U_{wmax}	5L/min

3. 3. Open-Loop Response

The model equations developed in the chapter 2 were discritized and the resulting equations were solved using finite numerical method. First, the open loop responses of the RFH system subject to constant outdoor temperature of -5°C with constant control inputs U_b=0.2, U_w=0.5 are depicted in Figure 3.3.1. The intent of this simulation test run was to establish the order of magnitudes of steady state time of the system temperature responses.

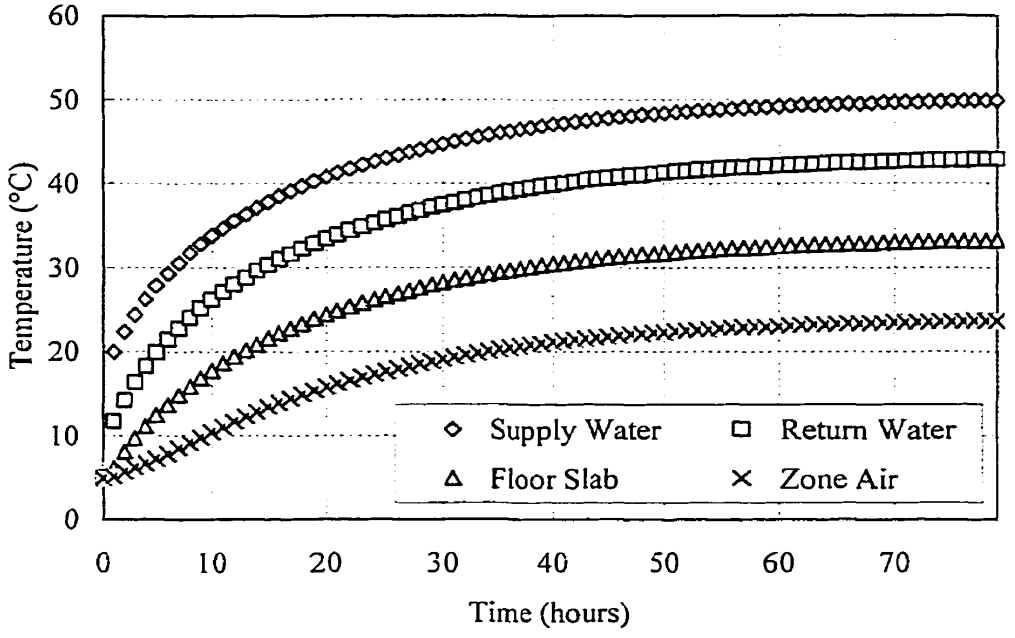

Figure 3.3.1 Open loop responses of the system

The slow response of the system is indicative of large thermal capacity of the room. With no control and the boiler running at low capacity nearly 50 hours are needed for the system to reach steady state. Under steady state condition the temperatures

reached the following values, zone air temperature T_z=23°C, floor slab surface temperature T_{sl} =33°C, supply water temperature T_{sp}=50°C and return water temperature T_{rt} =43°C.

The results show the expected tends of a system undergoing heating giving rise to exponential responses, which asymptotically attain steady state. Note that the temperature of floor surface is 10°C lower than the temperature of return water. The difference between supply and return water temperatures is 7°C. The floor slab temperature is 10°C higher than room air temperature. These temperature distributions, which may not be optimal but they exhibit expected trends and are with in the range reported in literature. This gives a first indication that model equations, the computer code and solution technique used is yielding expected trends.

3. 4. Model Validation strategy

The objective of the experimental results presented in reference [8] were to compare the performance of two control strategies, namely, (i) slab temperature on-off control and (ii) two-parameter on-off control (TPC), with the widely used zone air temperature on-off control. For instance, the performance of air temperature on-off control implemented in Room A (Figure 3.2.1) was compared with slab temperature on-off control scheme implemented in Room B.

For the purpose of model validation in this thesis, several sets of experimental data under various operating and control schemes were chosen with a view to cover the entire range of data available. Therefore, in the following model predictions are compared with experimental data corresponding to all three control strategies.

(i) Air temperature on-off control: room thermostat controls the hot water valve in on-off mode.

(ii) Slab temperature on-off control: in this scheme slab surface temperature is used to control the hot water valve.

(iii) Two-parameter control: in this strategy both air temperature and slab surface temperature are used to control the valve sequentially using a preset switching time interval.

Thus, these control strategies were incorporated in the developed model and simulation runs were made under the same weather data and operating conditions as those used in the experiments. As this point it is noted that several initial trials were needed to arrive at a reasonable magnitude of the thermal capacity of the floor slab, the boiler and the rooms which satisfied all test results. Choosing an optimal value for these three parameters remains a challenging problem in validation/calibration studies. The "good numbers" for these parameters arrived by trial-and-error are given in Table 3.2.1 to 3.2.3. Incorrect magnitudes of these parameters significantly affect the number of daily on-off cycles and the shape of the temperature responses. In the following the results obtained from the simulation of each of the three control strategies are discussed.

3. 5. Room Air Temperature On-Off Control

The experimental data shown in Figure 3.5.1 corresponds to March 16, 1995. On this day the outdoor minimum and maximum air temperatures were -5°C and 7.5°C. For this test the room thermostat limits were set at 21°C (low limit) and 23°C (high limit) respectively.

The predicted responses from the model using the same 24-hour weather data and under similar operating conditions are plotted in Figures 3.5.1 and 3.5.2. It is apparent from the figures that the slab temperature and air temperature responses match closely with experimental data. A slight mismatch between 10:00 and 16:00 is due to errors in thermal capacity parameters as well as solar transmission load from the enclosure as discussed earlier. In all simulations one single set of thermal capacity parameter satisfying all experimental results were chosen. For this reason there is some difference in predicted and measured data. But these differences are not significant.

The biggest difference in experimental and predicted temperatures taking place at noon with 1°C in zone air temperature and 3°C in slab temperature.

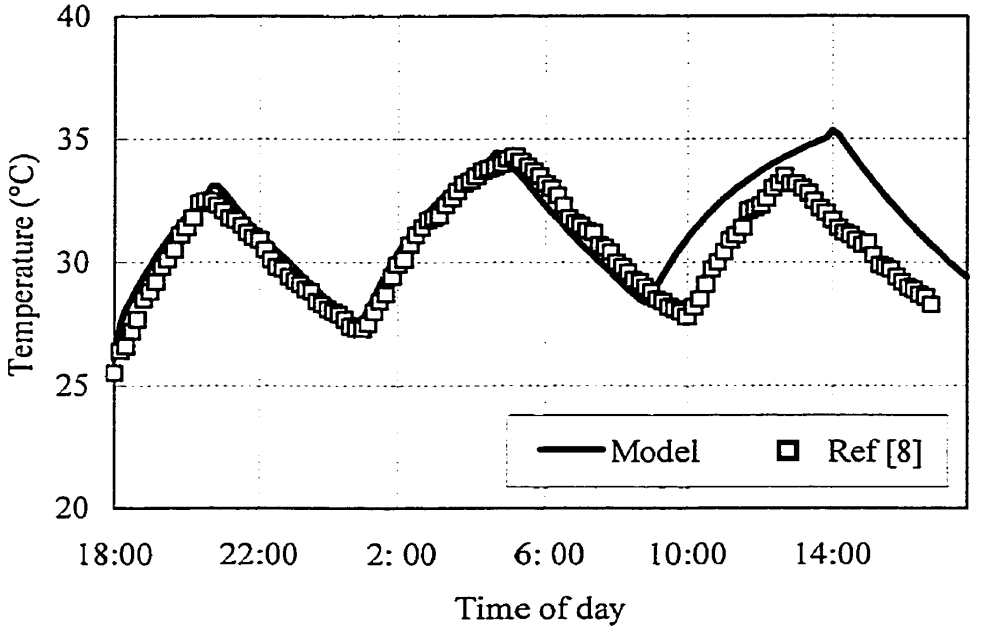

Figure 3.5.1 Predicted and measured floor slab temperature (air temperature control)

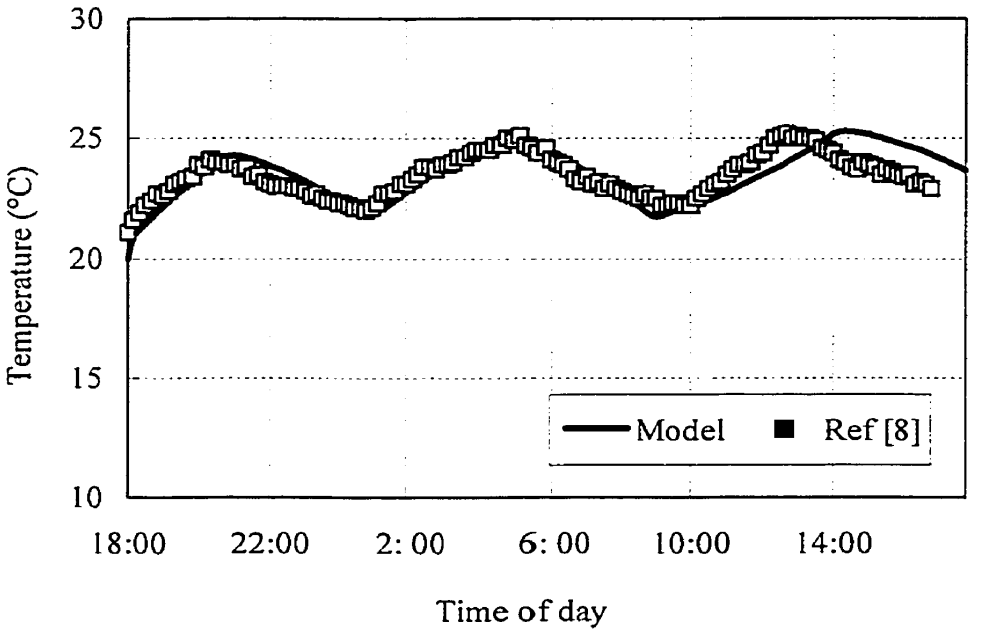

Figure 3.5.2 Predicted and measured air temperature (air temperature control)

3. 6. Floor Slab Temperature On-Off Control

For the same day (March 16, 1995) the system was controlled by floor slab surface temperature in room B. The slab thermostat was set at 29°C (low limit) and 31°C (high limit) respectively. The actual variations in slab temperatures were measured between 29°C and 32°C. The air temperature, which was allowed to float, varied about 22°C±0.75°C. The measured responses are plotted in figures 3.6.1 and 3.6.2 and compared with model predictions.

The results show that the model predicts the same number of on-off cycles as the measured data. The differences between the predicted and experimental responses are within ±2°C throughout the day.

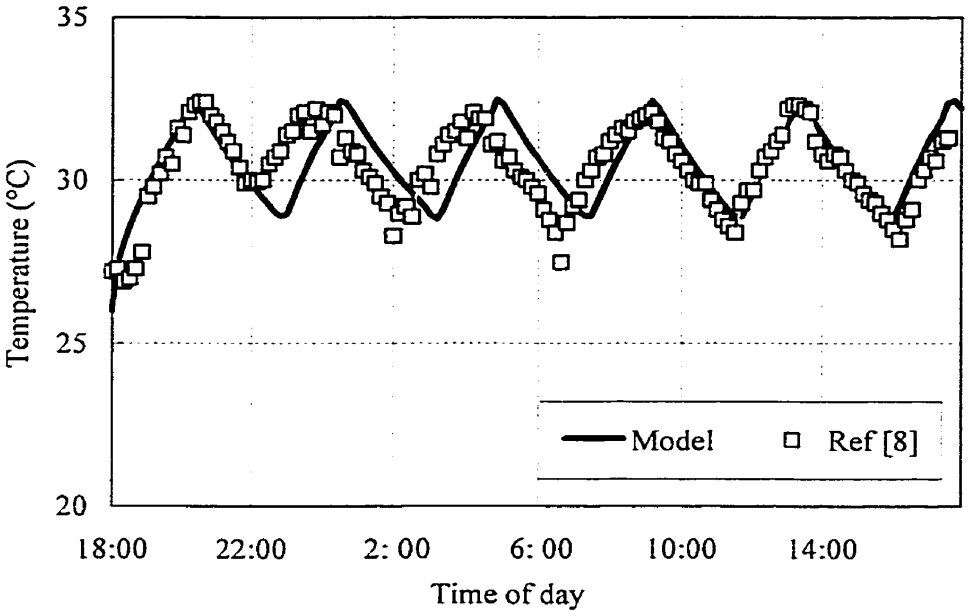

Figure 3.6.1 Predicted and measured floor slab temperature (slab temperature control)

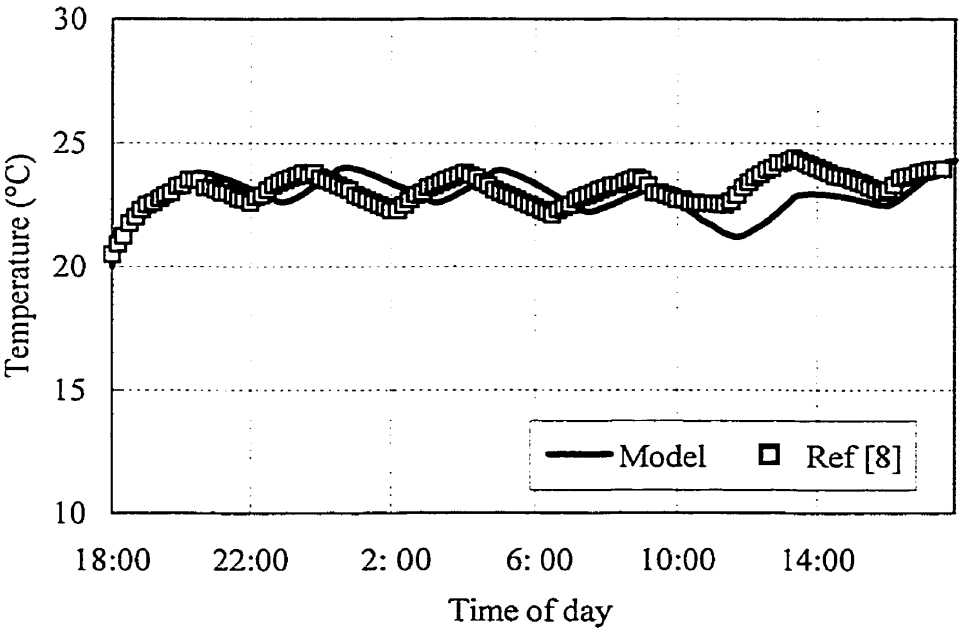

Figure 3.6.2 Predicted and measured air temperature (slab temperature control)

3. 7. Two-Parameter Control (TPC)

The TPC strategy combines both air temperature on-off control and slab temperature on-off control. In TPC air temperature control and slab temperature control works alternately and switches from one to the other with a preset switching interval. In the following the comparisons were made using the experimental results corresponding to three different switching intervals set at 10, 20 and 30 minutes each.

The results corresponding to 10 minutes switch interval are compared in Figure 3.7.1 and 3.7.2. Again we note that the model predictions compare well with experimental results.

Similarly, results of the comparisons with 20 minutes as switching interval are depicted in Figures 3.7.3 and 3.7.4.

The solid lines in the figures are the simulation results and experimental data in plotted as discrete point (square). Very good match indeed obtained even through the same value of thermal capacity parameters was used in these simulations.

Finally, the results with a switching interval of 30 minutes are plotted in Figures 3.7.5 and 3.7.6. The results correspond to a day in February 27, 1996.

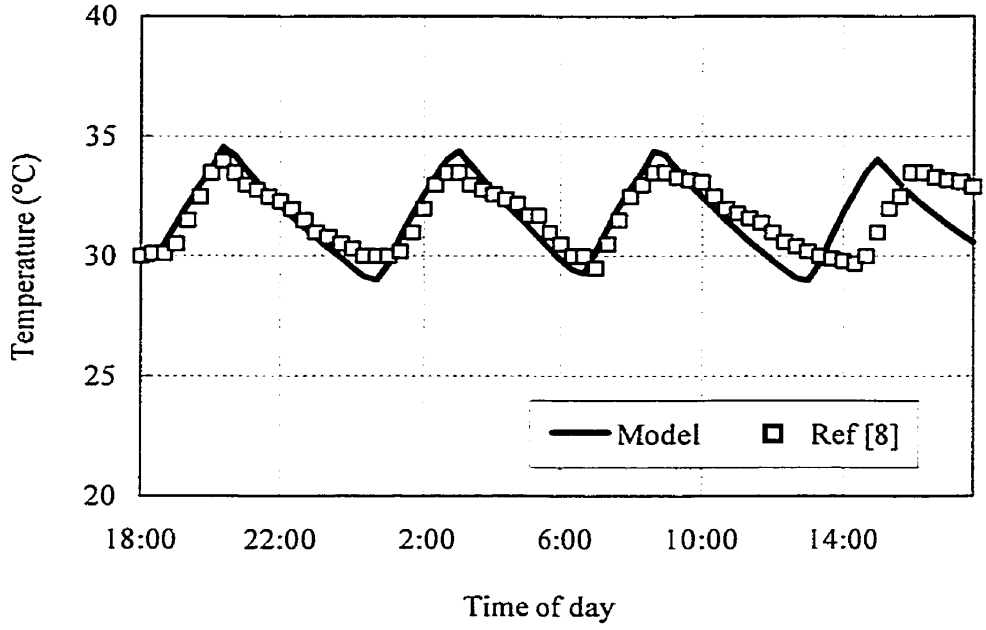

Figure 3.7.1 Slab temperature responses on March 13 with 10 minutes switching interval

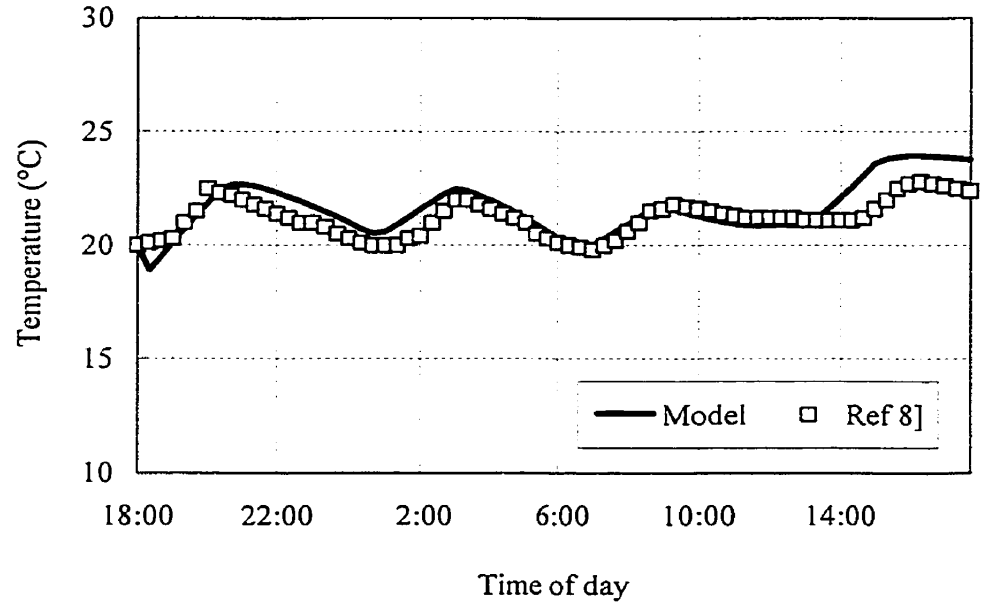

Figure 3.7.2 Zone air temperature responses on March 13 with 10 minutes switching interval

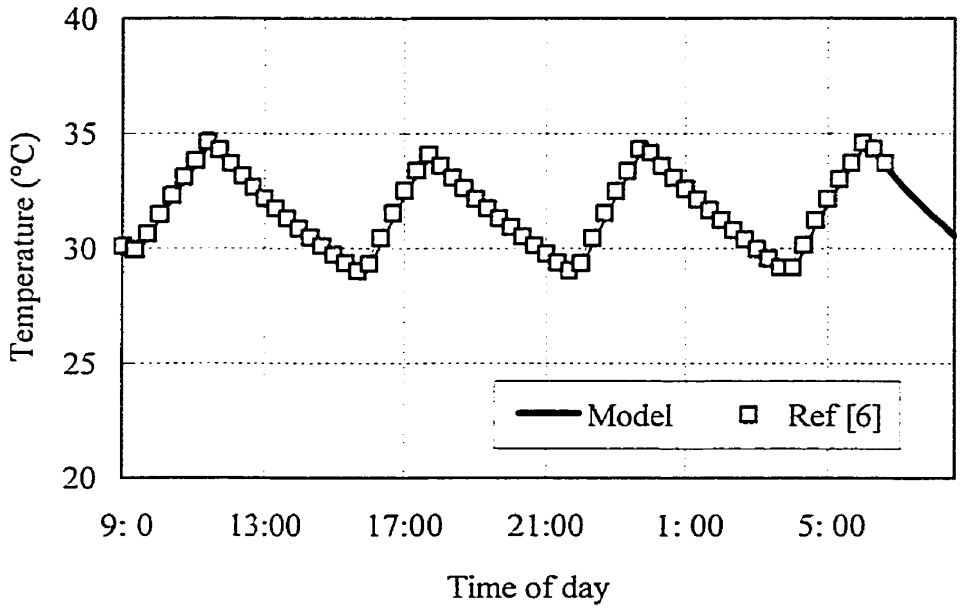

Figure 3.7.3 Slab temperature responses on Feb. 25 with 20 minute switching interval

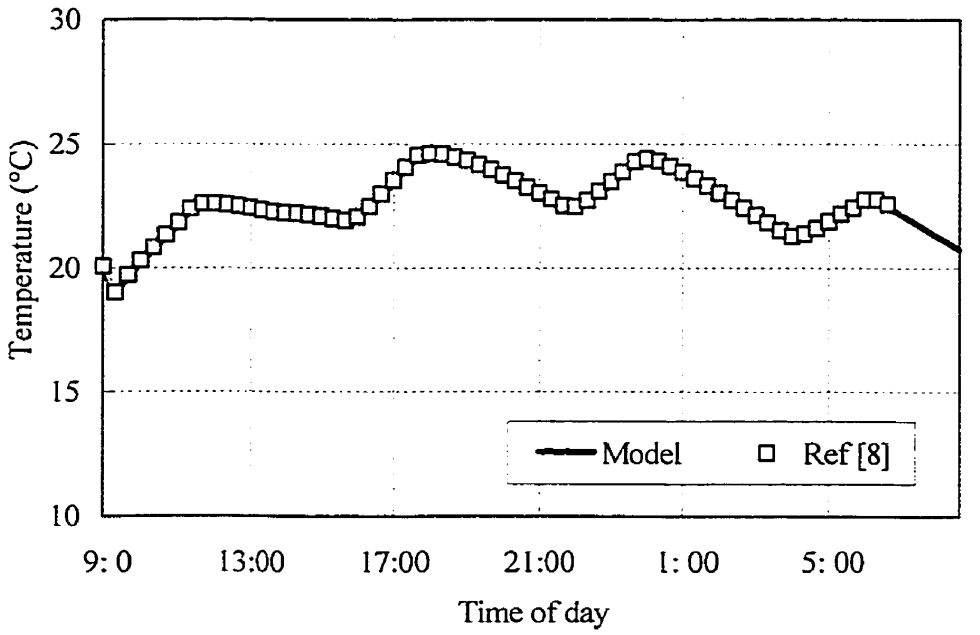

Figure 3.7.4 Zone air temperature responses on Feb. 25 with 20 minutes switching interval

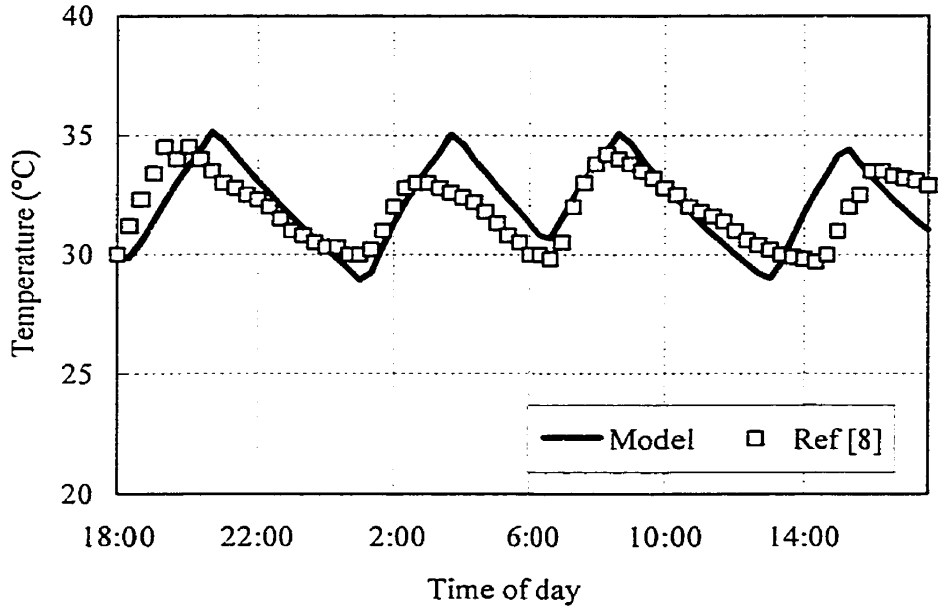

Figure 3.7.5 Slab temperature responses on Feb. 27 with 30 minutes switching interval

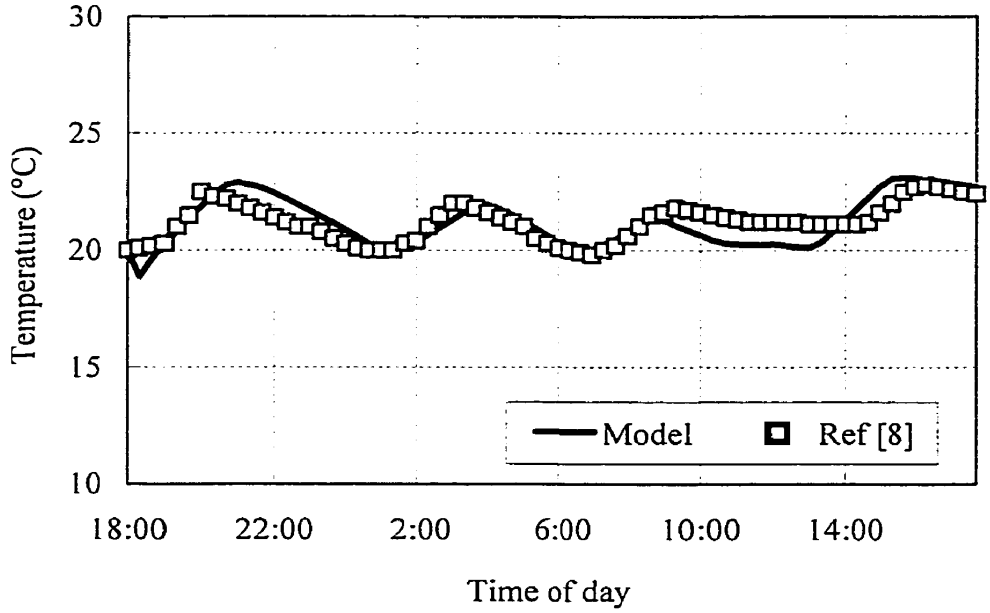

Figure 3.7.6 Zone air temperature responses on Feb. 27 with 30 minutes switching interval

A maximum error of 3°C in the slab temperature responses can be noted from Figure 3.7.5, which is the highest among all the comparison made thus far.

3. 8. Summary

The overall model was verified with experimental data from several different days covering a range of weather conditions corresponding to typical from normal to warm days of the heating season. Also the sets of data represented various operating control strategies such as conventional on-off control, floor slab temperature on-off control and two-parameter on-off controls. Comparisons between predictions and experimental data show good agreement with regard to daily dynamic variations in predicting occupied zone temperatures.

The simulation results agree well with the test data. Most of time the differences between the simulation and the test data are less than 1°C in both zone air temperatures and slab temperatures. The differences tend to be somewhat higher at noon with up to 2°C in zone air temperature and 3°C in slab temperature. This is attributed to some error in exactly matching the thermal capacity effects and its response due to transmission component of solar radiation through enclosure walls and ceiling. However these differences are not very significant.

Therefore, we conclude that the simulations from the model are in general agreement with the experimental data. As well the predicted number of on-off cycles

match well with the measured responses. Thus the model is able to closely predict the trends and daily responses and thus can be taken as a reliable tool for exploring and developing control strategies for improving the performance of RFH system.

CHAPTER 4

MULTI-STAGE CONTROL STRATEGIES

4. 1. Introduction

In this chapter a multistage control method, which is expected to improve the temperature regulation performance of a RFH system, will be developed. The major objective of the control strategy to be developed is that it should be the simple and effective and give good temperature control. First we review some of the critical issues in a RFH control.

An estimated $100 W/m^2$ of energy is transferred from a RFH system under typical operating conditions. Slightly greater than one-half of this energy is transmitted in radiant mode and the rest in convective mode. Not only the mode of heat transfer but also the thermal lag effect associated with radiant floor slab pose a challenging control problem and thus require innovative solutions. In recent studies researchers have examined outdoor reset control strategies (Leigh, 1991 [20]; MacCluer, 1991 [23]); on-off, PI (proportional-integral) and two-parameter control schemes (Cho and Zaheer-Uddin, 1997 [8]) in houses heated with RFH systems. Although PI controllers with or without outdoor air reset strategy give better temperature control, they are relatively expensive. To this end, there is a need to develop simple and yet cost effective control strategies for RFH systems. In this regard, two-parameter control (TPC) strategy [8] has been shown to be simple and effective control for RFH systems. In TPC, zone air and slab temperature

signals are used in alternate sequence for on-off control of the pump or valve. By so doing, it was found that temperature swings in floor-slab and zone-air temperature were reduced compared to single parameter control (SPC) in which only zone air temperature was used as a feedback signal for on-off control of the pump or the valve.

Although TPC gives good temperature regulation, problems still remain in the installation and the location of slab temperature sensors in the floor slabs especially in multi-room houses. It is in this context we are interested in seeking an alternative control scheme.

Rather than operating the water valve in full on or completely off mode, it is proposed to cover the total control range in few stages based on the air temperature as a feedback signal since most systems still rely on room thermostat for temperature control. As the number of stages are increased, the multistage control responses are expected to approach those of a proportional control. It is however recommended limiting the number of stages between two to four from the viewpoint of the ease of implementations.

In this chapter a multi-stage control (MSC) strategy for RFH systems will be explored. The MSC is expected to have good temperature regulation properties without requiring the slab temperature as feedback signal. The following methodology will be used to examine the effectiveness of MSC strategy:

1) Compare the effect of mass flow rate control (constant supply water temperature) versus the effect of supply water temperature control (constant

water flow rate) on the zone temperature responses and select the most effective control variable.

2) Compare the temperature responses of RFH system with MSC and TPC under several different operating conditions.

4. 2. Sensitivity of Control Parameters

There are two ways to control a RFH system by changing either supply water temperature or supply water mass flow rate. In order to control the system more effectively, it is necessary to examine the effect of these two control inputs on the temperature responses of the RFH system.

To examine the effect of varying the water mass flow rate the following operating conditions were chosen: outdoor temperature -10°C, supply water temperature at 50°C. The mass flow rate of water was varied from 25%, 50% and 100% of the rated pump capacities of 5L/min and 3L/min. The resulting zone air temperature responses are plotted in Figures 4.2.1a and 4.2.1b.

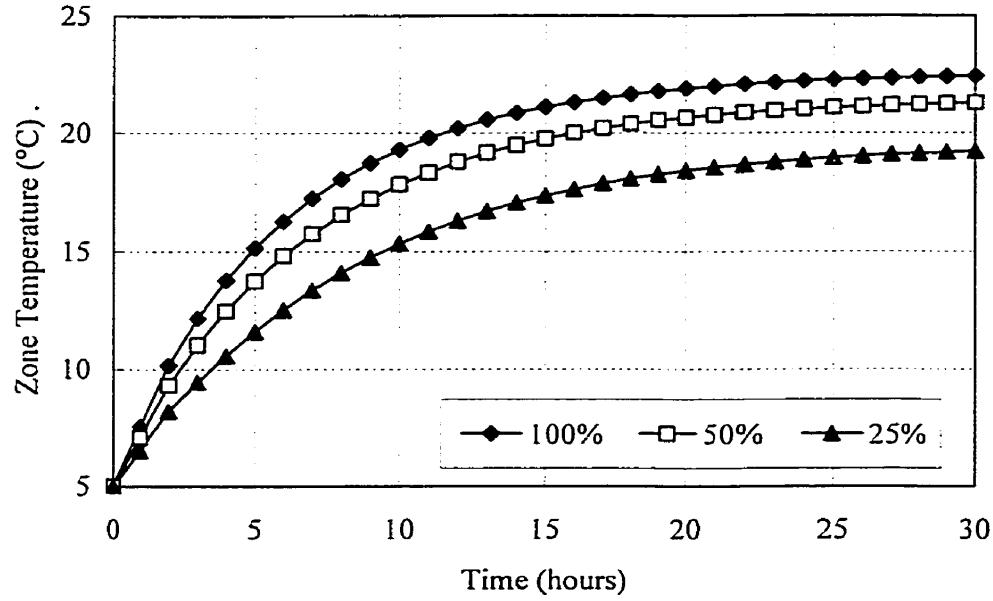

Figure 4.2.1a Effect of water mass flow rate (pump capacity = 5L/min)

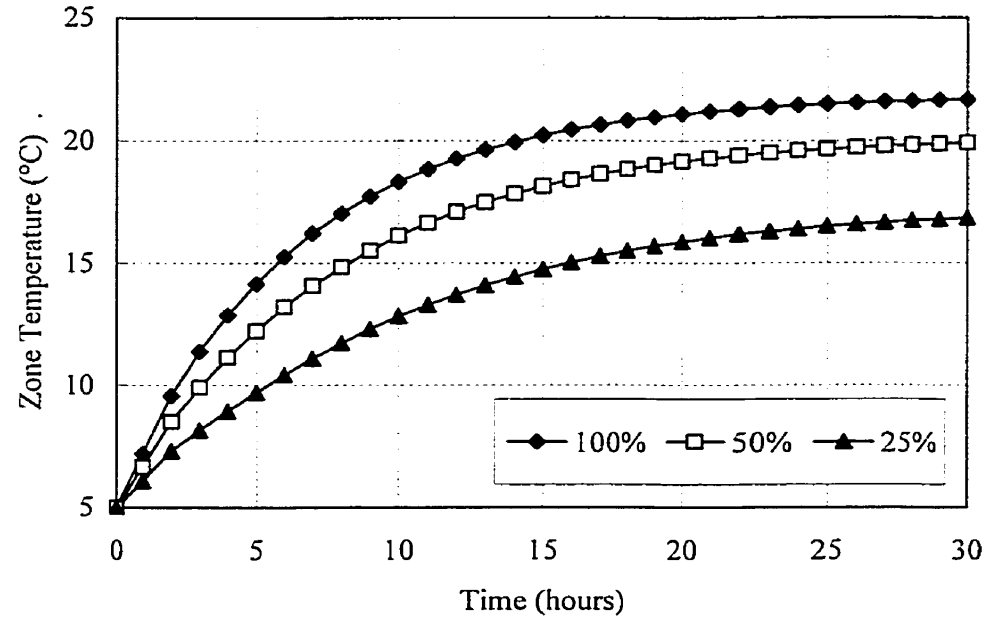

Figure 4.2.1b Effect of water mass flow rate (pump capacity = 3L/min)

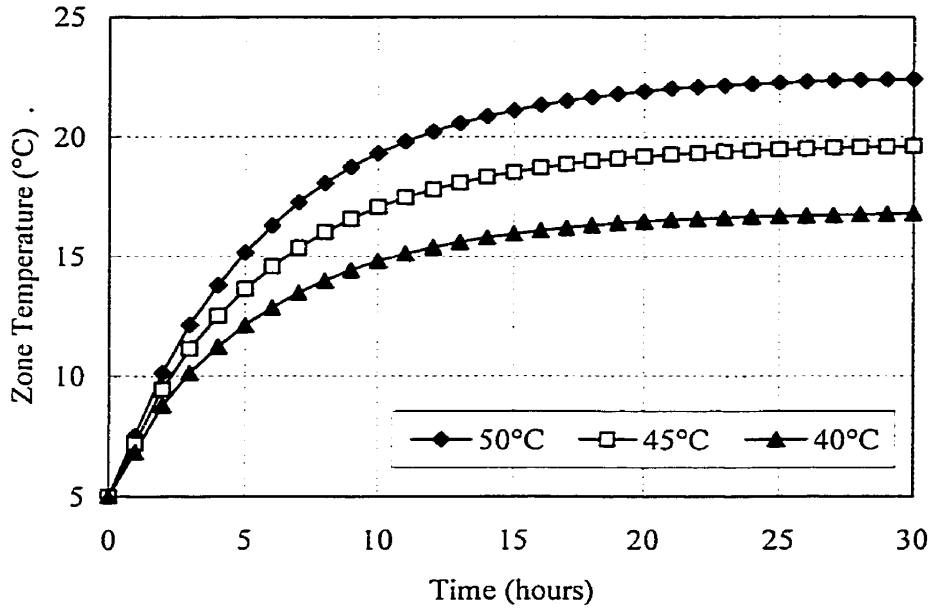

Figure 4.2.2a Effect of water temperature with 5L/min

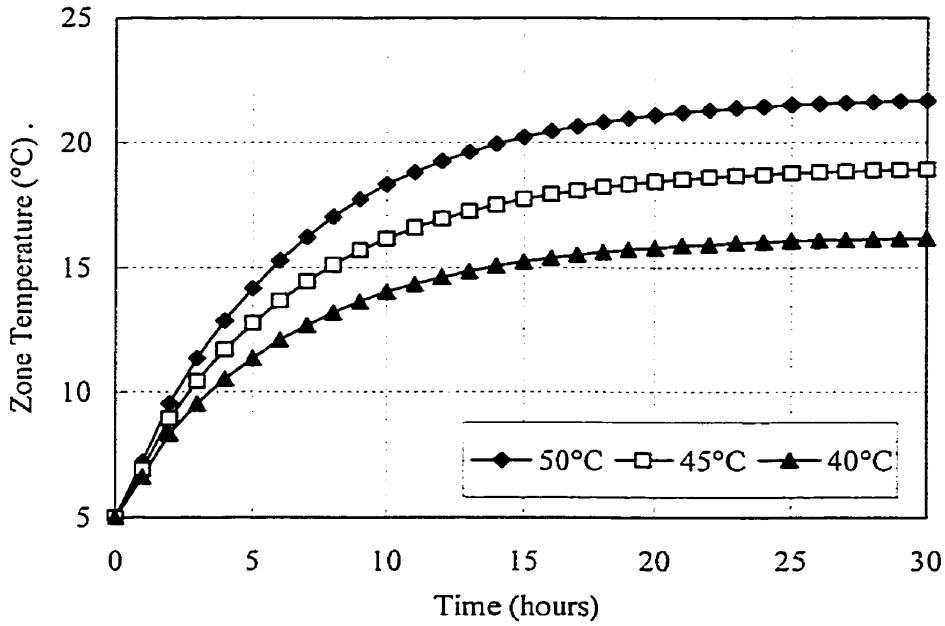

Figure 4.2.2b Effect of water temperature with 3L/min

To study the effect of supply water temperature, the RFH system responses were simulated under the same operating conditions as noted above. Two different water mass flow rates of 5L/min and 3L/min were used. In each case the supply water temperature was held constant at 50°C, 45°C and 40°C respectively. The zone air temperature responses are shown in Figures 4.2.2a and 4.2.2b.

It is apparent from these responses that an effective control strategy will be the one utilising water temperature modulation as opposed to flow rate modulation. For example, the results show that a 5°C increase in supply water temperature causes about 3.5°C rise in zone air temperature. On the other hand a 50% increase in mass flow rate increases the zone air temperature by only 0.5°C. Therefore, it is advantageous to use supply water temperature modulation strategy to control RFH systems. However, is will be interesting to study the effect of both temperature and flow rate modulation, one at a time, in a closed loop control mode.

Figures 4.2.3a and 4.2.3b show the schematic diagram for implementing the flow rate and temperature modulation control strategies. As shown in Figure 4.2.3b by connecting the diverging three-way valve downstream of the pump, the supply water temperature to the floor slab is changed since boiler temperature and return water temperature are mixed in different proportions in responses to the zone air temperature signal. The control range of the three-way valve (0 to 100%) could be modified to cover in two (0-50%-100%) or four (0-25%-50%-75%-100%) stages. Depending on whether the three-way valve is in mixing mode or diverging mode the supply water temperature or

mass flow rate to the floor slab changes accordingly. In the following the multistage control strategy will be defined and results obtained from the simulation runs will be presented.

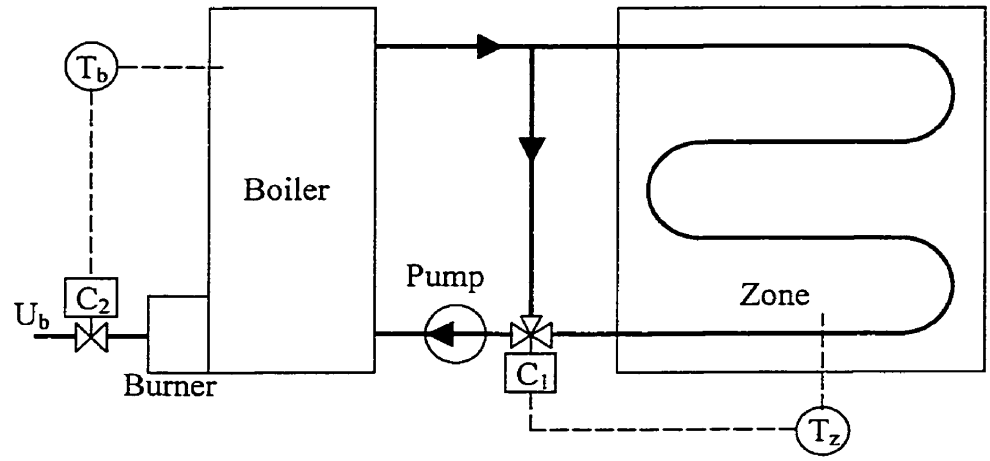

Figure 4.2.3a Three-way valve arrangement for mass flow modulation

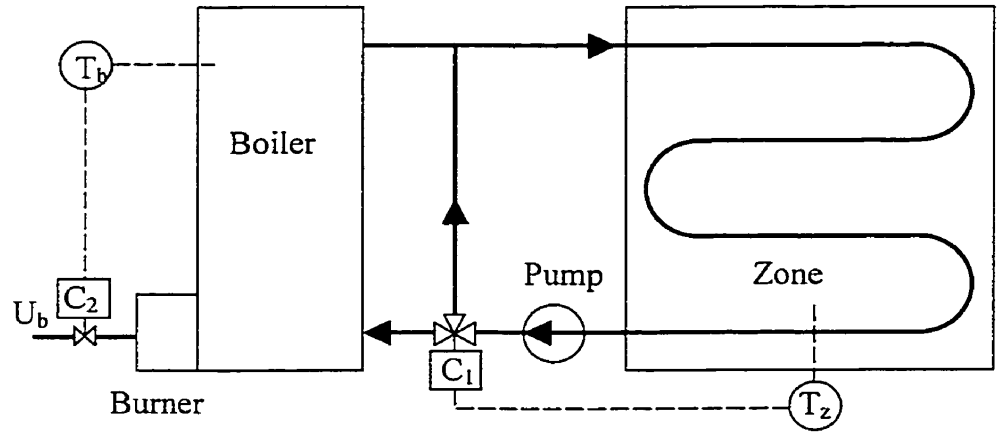

Figure 4.2.3b Three-way valve arrangement for supply water temperature modulation

4. 3. Two-Stage Control Strategy

A two-stage control strategy was defined as follows.

$$\text{If } T_z \geq T_{max}; \qquad \dot{m}_s = 0.0, \dot{m}_b = 1.0,$$

$$\text{If } (T_{max}\text{-}0.75TR) < T_z \leq (T_{max}\text{-}0.25TR); \qquad \dot{m}_s = \dot{m}_b = 0.5,$$

$$\text{If } T_z < T_{min}; \qquad \dot{m}_s = 1.0, \dot{m}_b = 0.0,$$

Where $\dot{m}_s$ is the mass flow rate of supply water to the floor slab, $\dot{m}_b$ is the bypass water mass flow rate. T_{max} and T_{min} are high and low limits of zone thermostat setting and TR is the throttling range. For example, with T_{max} = 23.0°C and T_{min} = 21.0°C, the control strategy works as follows. When the zone temperature is greater than 23.0°C the supply water to floor slab is turned off (bypass valve is fully open). On the other hand, when zone temperature falls below 21.0°C, the supply water to the floor slab is at its maximum while the bypass is closed. An intermediate stage which enhances the performance of this control strategy is activated when the zone temperature remain between 21.5°C to 22.5°C range. In this case, the three-way valve is set to open the supply and bypass ports equally. Thus by mixing equal portions of boiler water and return water, the temperature of supply water to the floor slab is modulated.

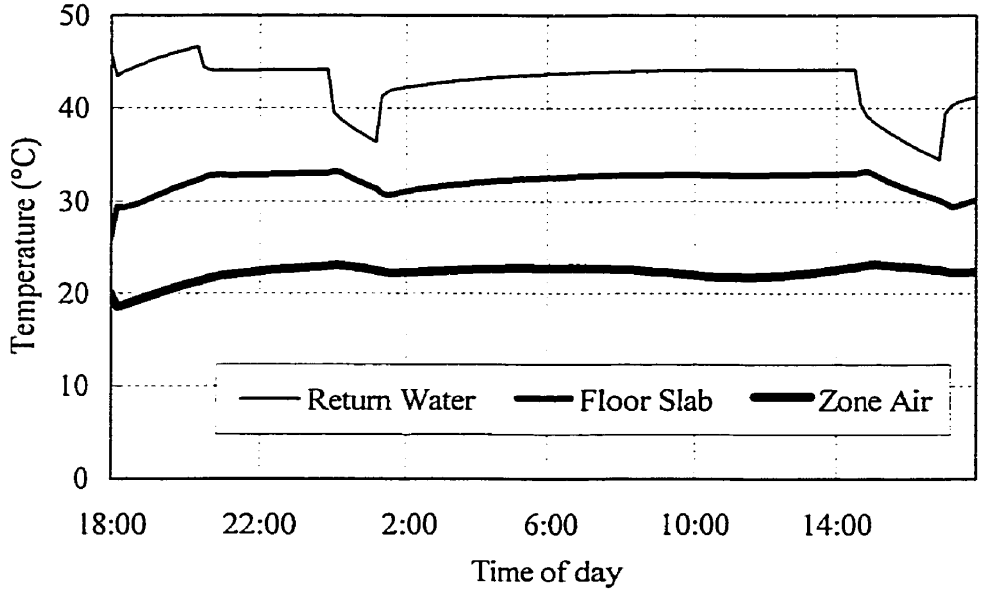

Figure 4.3.1 TSC-TM without solar and internal heat gain

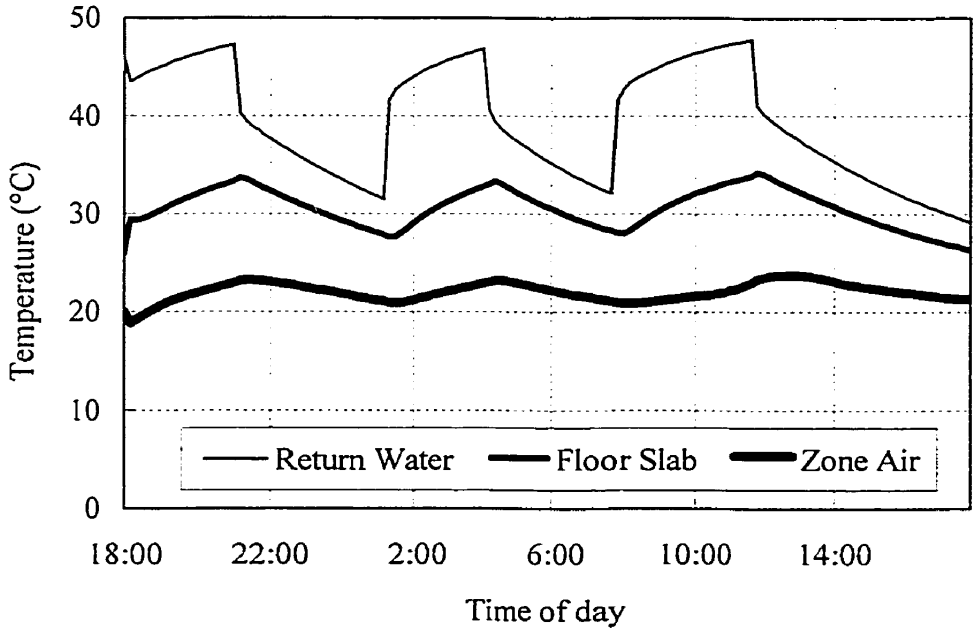

Figure 4.3.2 SPC without solar and internal heat gain

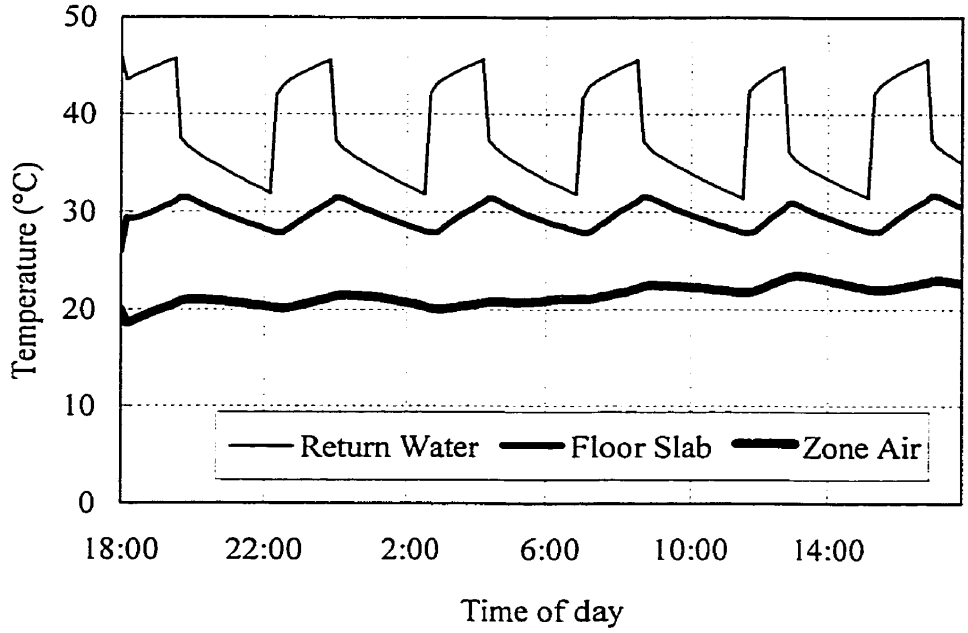

Figure 4.3.3 TPC without solar and internal heat gain

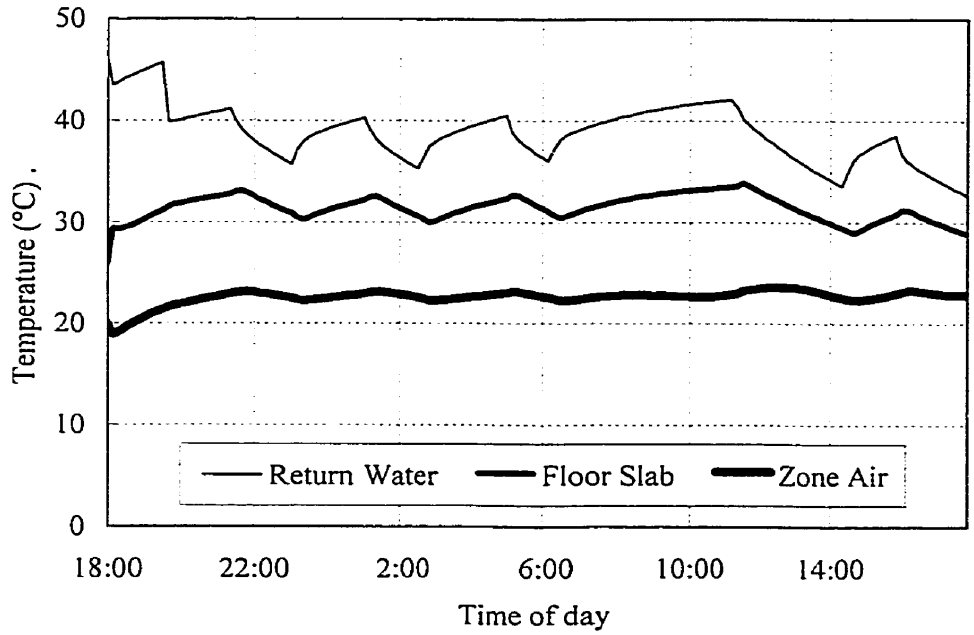

Figure 4.3.4 TSC-MM without solar and internal heat gain

Shown in Figures 4.3.1 to 4.3.4 are the responses obtained with the two-stage control with temperature modulation (TSC-TM), two-stage control with supply water mass flow rate modulation (TSC-MM), single-parameter air temperature control (SPC), and the two-parameter control (TPC) schemes. In each case, room air temperature is used as the feedback signal. The high and low setpoint limits were defined as 23.0/21.0°C. In TPC the slab temperature limits were set as 31.0/28.0°C. Solar radiation, outdoor air infiltration and internal heat generation were not taken into account in the simulation runs. Simulation runs were carried out on a day with outdoor air temperature varying in between -5°C to 7°C. The hot water temperature from the storage tank was assumed to be constant at 57°C. The initial conditions were assumed as follows: zone air temperature = 20°C, enclosure surface temperature = 20°C, floor slab surface temperature = 27°C and return water temperature = 45°C.

It is apparent from Figure 4.3.2 that the air and slab temperature experience significant swings (20.5/24.0°C and 34.0/28.0°C) with the conventional zone air temperature based on-off (SPC) control. On the other hand the introduction of staging significantly improves the slab temperature responses. For example, the maximum and minimum limits obtained with two-stage (TSC-TM) control are (Figure 4.3.1): slab temperature = 33.0/29.5°C and room air temperature = 21.5/23.0°C. It also far better compared to the TPC (Figure 4.3.3), which results in variations in air temperature of 24.0/20.0°C and in slab temperature between 27.5/31.5°C. The temperature responses with two-stage control using supply water mass flow rate regulation (TSC-MM) are

shown in Figure 4.3.4. Again it is apparent that temperature modulation results in slightly better control.

In order to assess the performance of the two-stage control under realistic operating condition acting on the RFH system, the normal disturbances such as solar radiation, outdoor air infiltration and internal heat gain were included in the following simulation runs. A constant air change per hour (ACH) rate of 0.5 was used to compute the infiltration heat loss so that the infiltration heat loss is a functional of the outdoor air temperature. A typical internal heat gain profile (Barakat 1986) [6] was used to simulate internal heat gain of a dwelling that is depicted in Figure 4.3.5. The internal heat gain is up to about 400W during cooking time, 100W in the morning, 200W in the evening and 80W throughout the night. The solar radiation flux, which starts at 8 o'clock and reaches peak at noon in 250W/m^2 was used in the simulation runs.

Responses from Figure 4.3.6 with solar and internal heat gain show that the zone air and slab temperatures are maintained within the same range compared to the without internal and solar radiation responses curves in Figure 4.3.1. This shows that the TSC-TM strategy is robust in rejecting the disturbance effects. The corresponding TPC and SPC responses are depicted in Figure 4.3.7 and 4.3.8. Temperature responses obtained with TSC-MM strategy are shown in Figure 4.3.9. Note that TSC-TM control (Figure 4.3.6) while giving better temperature control also reduces the number of on-off switchings compared to the TSC-MM control strategy (Figure 4.3.9).

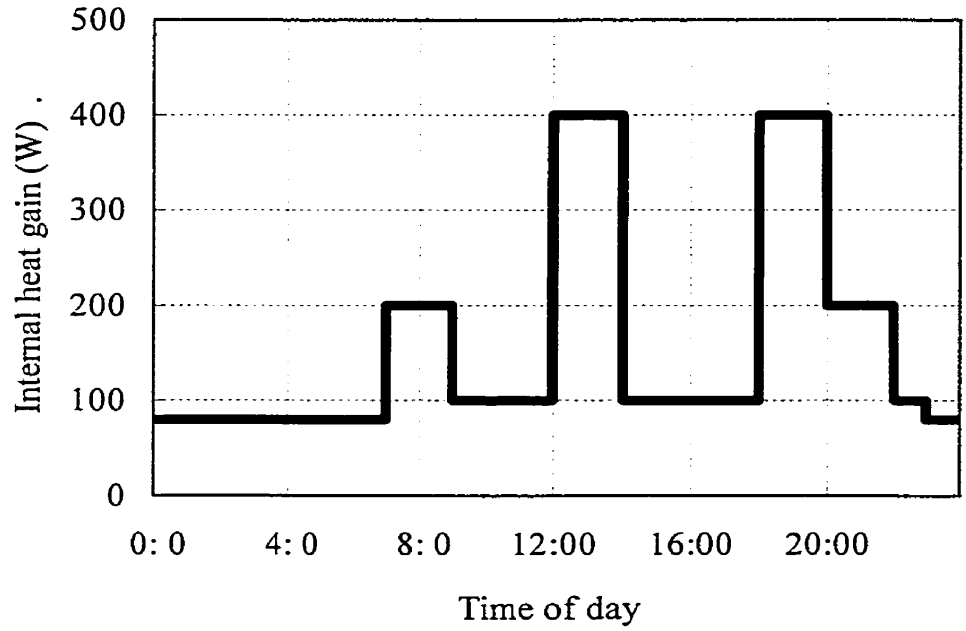

Figure 4.3.5 Profile of internal heat gain of a dwelling

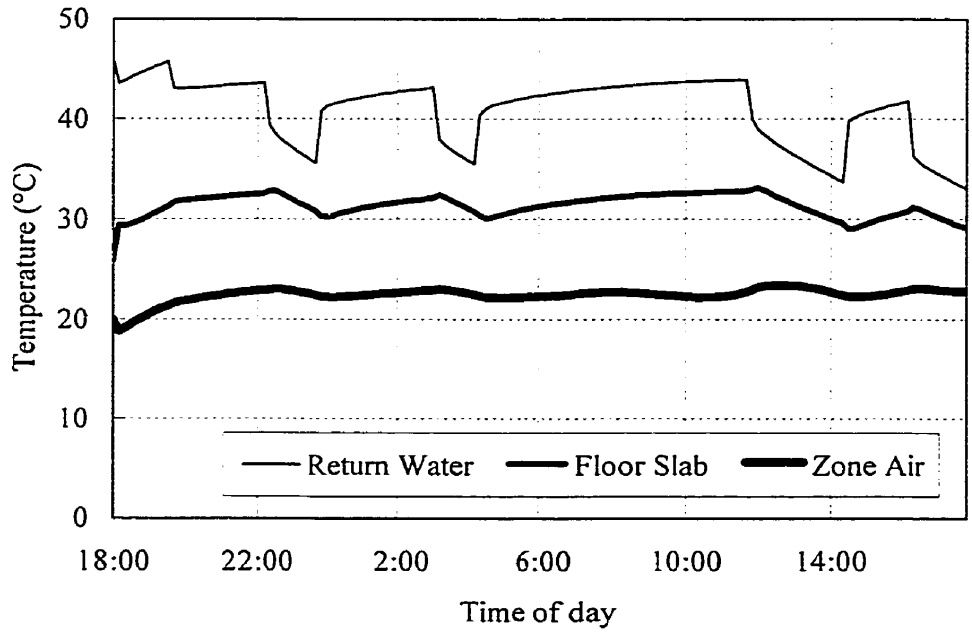

Figure 4.3.6 TSC-TM with solar and internal heat gains

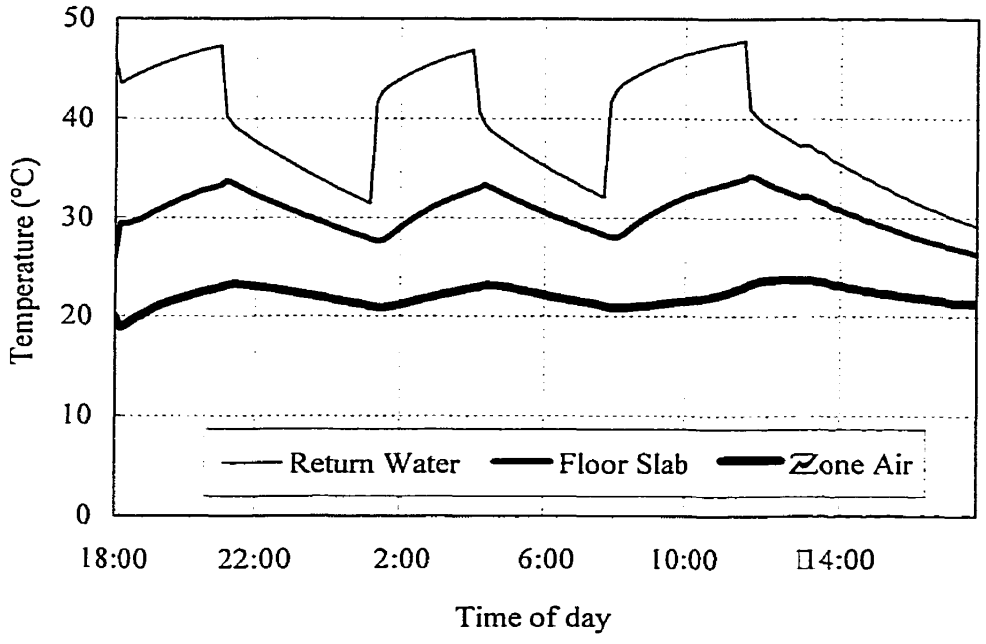

Figure 4.3.7 SPC with solar and internal heat gains

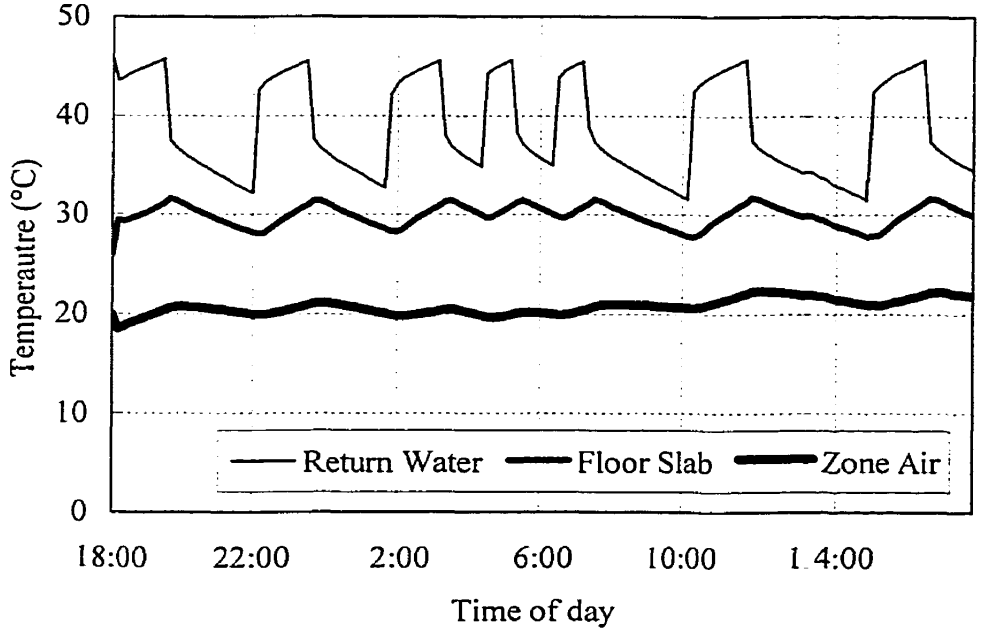

Figure 4.3.8 TPC with solar and internal heat gains

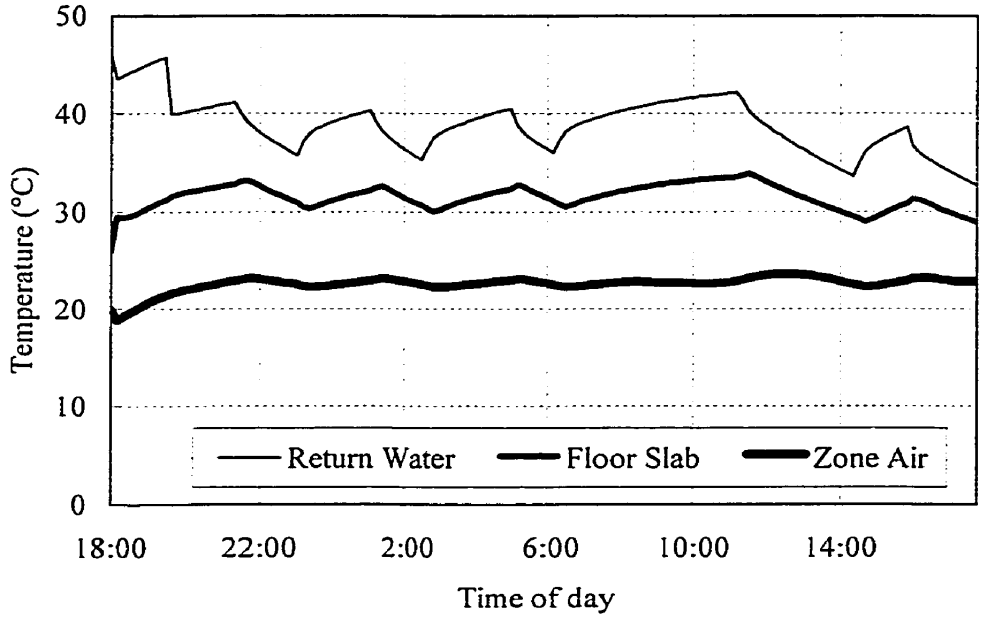

Figure 4.3.9 TSC-MM with solar and internal heat gain

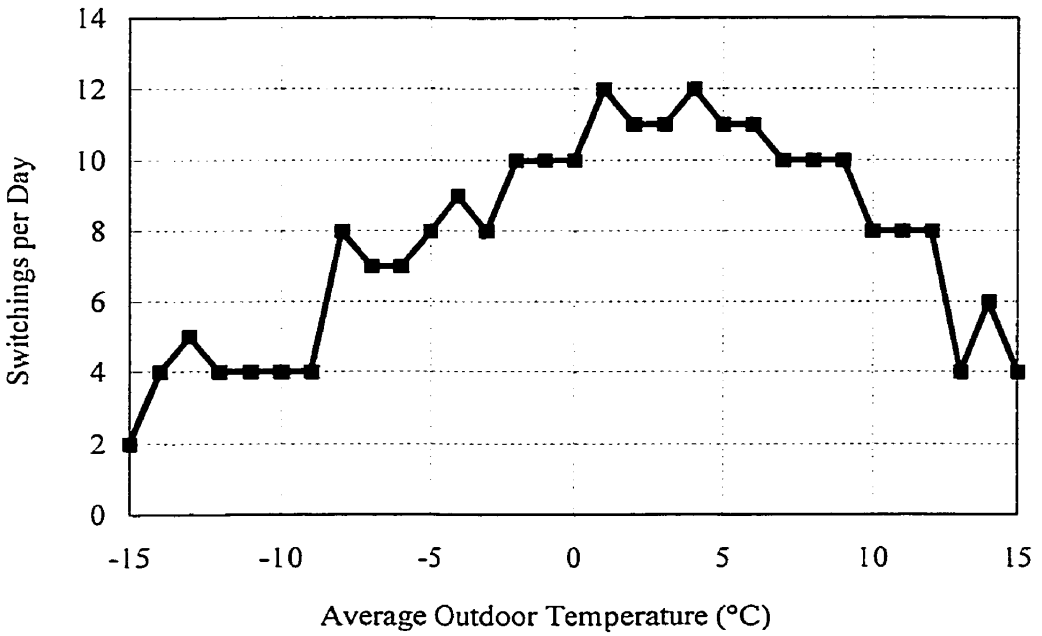

Figure 4.3.10 Potential number of switchings per day

From the simulation results predicted in Figures 4.3.1 through Figure 4.3.9 it can be noted that irrespective of the cold outdoor temperature conditions and internal heat gains the two-stage control (TSC) outperforms the on-off control (SPC) and gives good temperature regulation throughout the day.

From the point of view of implementing the two-stage control (TSC) a question arises as to the number of times per day the valve actuator will have to switch from one to other position. To quantify this effect we have simulated the two-stage control (TSC) operation on several days ranging from cold to warm weather conditions. Figure 4.3.10 shows the total number of switchings per day as a function of average outdoor temperature. It is apparent from the figure with the two-position control the actuator could experience between 10-12 switchings between stages per day. The results show that the number of switchings decreases under cold and warm weather conditions. This result cannot be generalised. However, it is intended to show the typical number of switchings per day under normal operating conditions.

4. 4. Four-Stage Control Strategy

Further improvements in slab and zone air temperature responses can be achieved by using four-stage control (FSC) as depicted in Figure 4.4.1 with temperature modulation (TM) and in Figure 4.4.2 with mass flow rate modulation (MM) respectively. These simulation runs were carried out using the same outdoor, slab and internal gain profiles as those used in Figure 4.3.3 and 4.3.4.

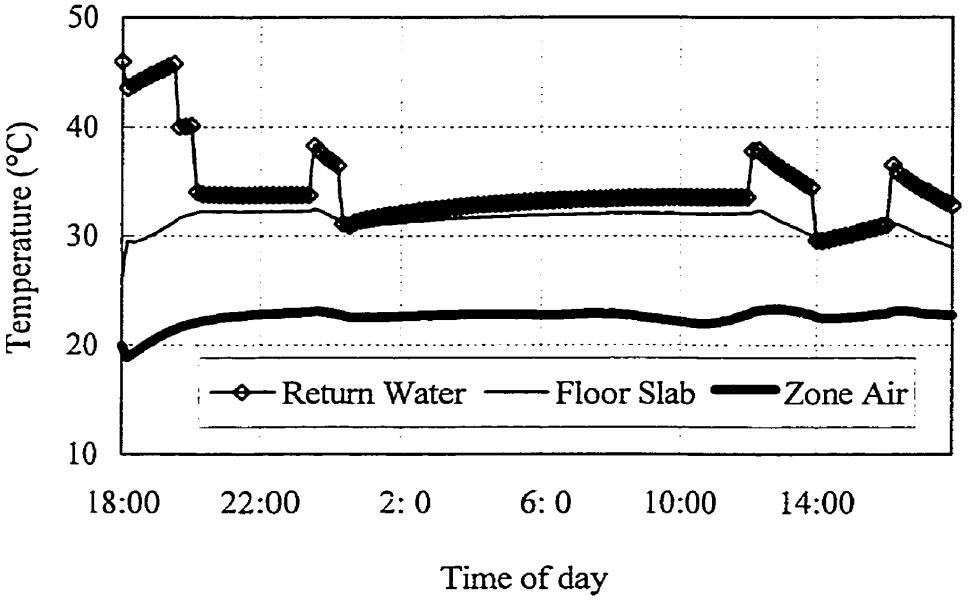

Figure 4.4.1 Four-stage control with mass modulation (FSC-MM)

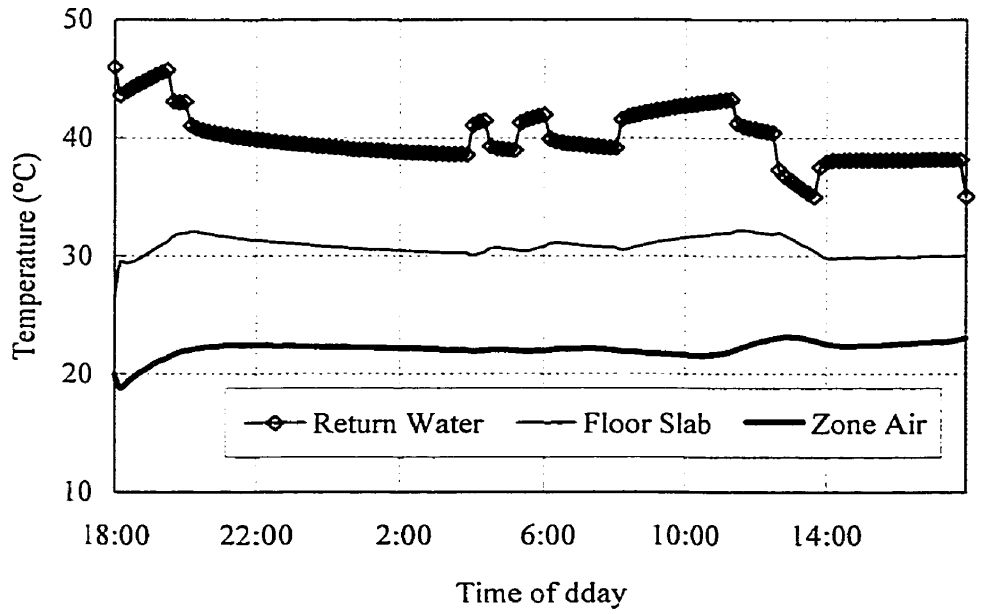

Figure 4.4.2 Four-stage with temperature modulation (FSC-TM)

The four-stage control (FSC) was defined as follows:

$$\text{If } T_z \geq 23.0^{\circ}C, \qquad \dot{m}_s = 0.00, \dot{m}_b = 1.00,$$

$$\text{If } 22.75^{\circ}C > T_z \geq 22.0^{\circ}C, \qquad \dot{m}_s = 0.25, \dot{m}_b = 0.75,$$

$$\text{If } 22.0^{\circ}C > T_z \geq 21.5^{\circ}C, \qquad \dot{m}_s = \dot{m}_b = 0.50,$$

$$\text{If } 21.5^{\circ}C > T_z \geq 21.0^{\circ}C, \qquad \dot{m}_s = 0.75, \dot{m}_b = 0.25,$$

$$\text{If } T_z < 21.0^{\circ}C, \qquad \dot{m}_s = 1.00, \dot{m}_b = 1.00,$$

The mixing water temperature entering the floor slab is given by:

$$T_{mix} = \frac{\dot{m}_s T_{sp} + \dot{m}_b T_{rt}}{\dot{m}_s + \dot{m}_b} \tag{4.3.1}$$

From the figures it is noted that the zone air temperature varies between high 23.5°C and low 22.5°C, and the floor slab temperature varies between 30.0°C to 32.5°C. Compared to the results obtained with two-stage control (TSC) earlier the four-stage control shows somewhat better performance in term of slab temperature. However, this advantage is achieved at the expense of increasing the complexity of control strategy.

4. 5. The Interactions between Boiler Control and the TSC

In this simulation results presented in Figure 4.3.1 through 4.3.9 it was assumed that a constant temperature of hot water from a heating source such as a storage tank is available. In practice, the hot water is heated in a boiler, which is also operated in an on-off mode to keep the boiler temperature between certain high and low limits. Thus, the

cyclic variations in the boiler water temperature are likely to interact with the TSC strategy. To examine these effects the following simulation runs were carried out.

The boiler control loop was simulated as follows. Once the circulating pump (3L/min in capacity) is turned on, a built-in thermostat of the boiler will detect water temperature sends a feedback signal to the controller C_2, shown in Figure 4.2.3a and b, to turn on the burner (5000W in capacity) and there onwards keeps the boiler water within 55/59°C. Thus with this control the boiler temperature varies between 55-59°C in an on-off cyclic mode.

The temperature responses of two-stage control in temperature modulating mode are plotted in Figure 4.5.1 in which slab temperature varies between 29/33°C and air temperature varies 22.0/23.5°C. The ranges are similar to those obtained with constant supply water temperature depicted in Figure 4.3.6. Similar observations can be made with respect to the results obtained with TSC-MM strategy. However the number of on-off cycles per day increase when storage tank (constant water temperature source) is replaced by the boiler. The figures in this section also illustrate that zone air temperature and slab temperature are not significantly different under TM of MM mode. The regulating mode seems to only change the return water temperature, up to 44°C in Figure 4.5.1a, and 42°C in Figure 4.5.2a. The burner operating cycle lasts about 3 minutes under maximum water flow rate and 1 minute under a flow rate of 50%. The temperature of supply water, which represents boiler water also, drops to 33°C when the pump is turned off for large duration due to heat loss through the boiler jacket.

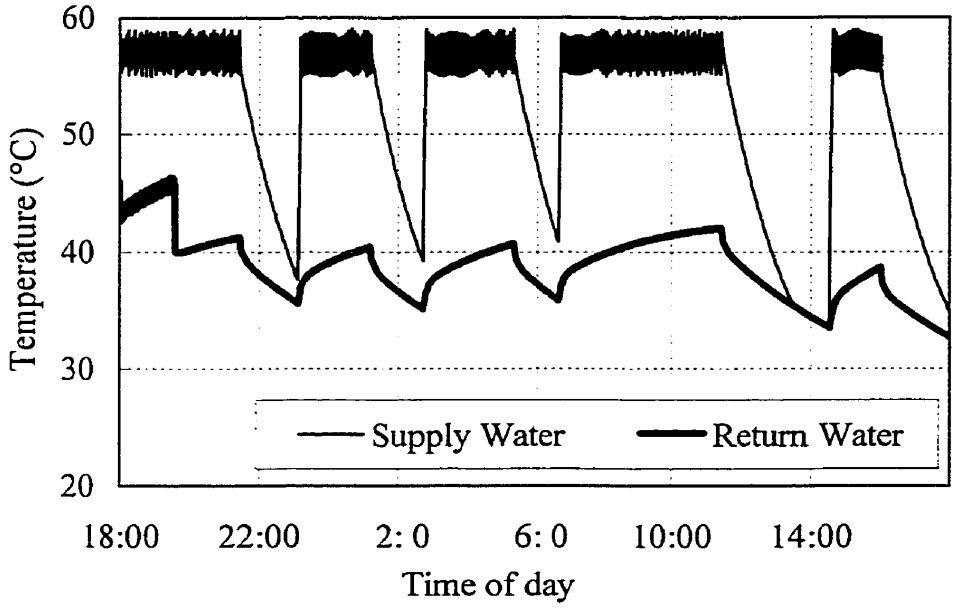

Figure 4.5.1a Boiler water temperatures with TSC-TM

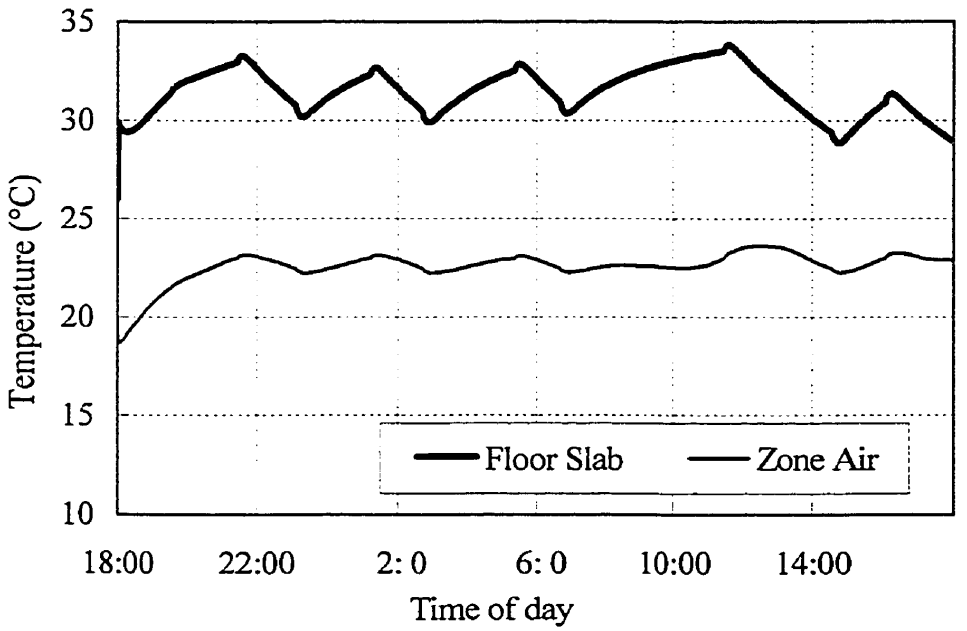

Figure 4.5.1b Air and slab temperature with TSC-TM

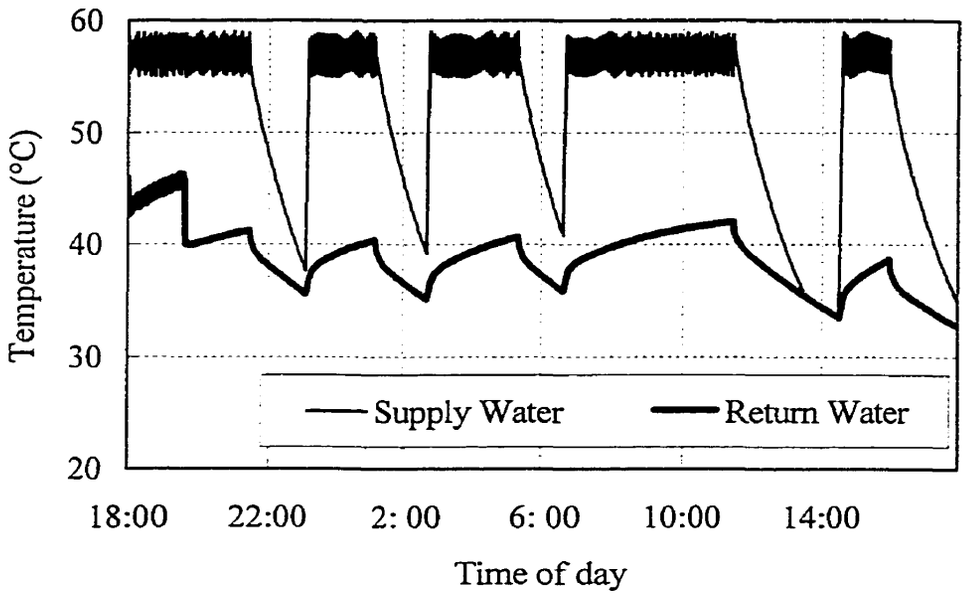

Figure 4.5.2a Boiler water temperatures of TSC-MM

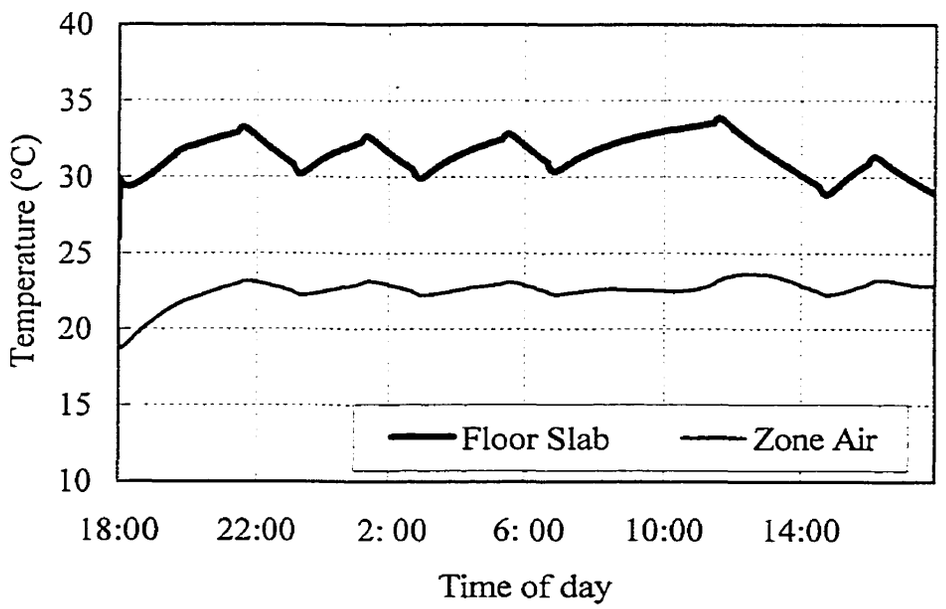

Figure 4.5.2b Air and slab temperatures of TSC-MM

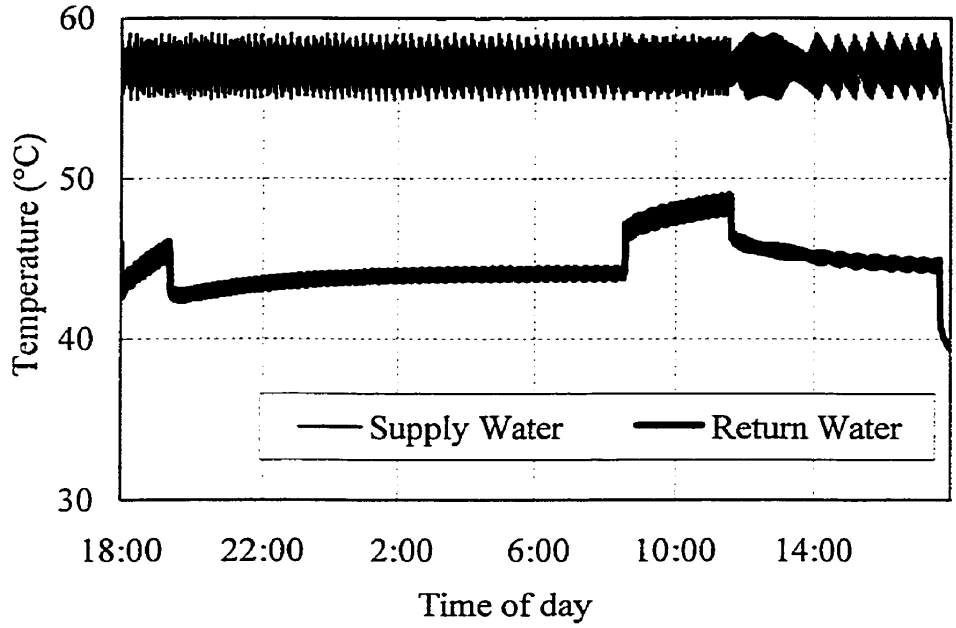

Figure 4.5.3a Boiler water temperatures with TSC-TM on a cold weather

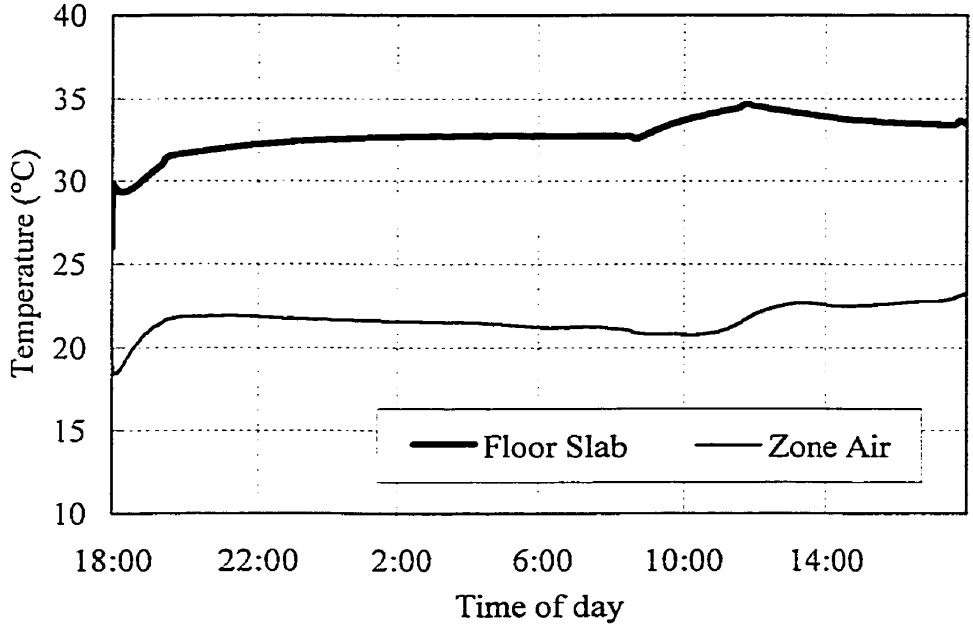

Figure 4.5.3b Air and slab temperatures with TSC-TM on a cold weather

A cold day weather condition (outdoor temperature -13/-1°C) was also simulated using TSC-TM mode with solar radiation, infiltration and internal heat gains. The results depicted in Figure 4.5.3 show that zone air is maintained between 21.0/23.0°C and the slab temperature between 32.5/35.0°C. From these results it can be noted that the two-stage control scheme can provide a stable control under a wide range of operating conditions.

4. 6. Summary

A multi-stage control (MSC) strategy, which uses zone air temperature as control signal and does not require the outdoor temperature and/or the slab temperature signals, has been developed. The performance of a RFH system can be improved by staging control variable to achieve either constant supply water mass flow rate with variable temperature (TM) or variable mass flow rate with constant temperature (MM). This study shows that TM as control variable has higher impact, such that constant mass flow rate with variable temperature might control a RFH system more efficiently. However, a constant temperature variable mass flow rate (MM) still offers the advantage in terms of saving pumping power. For a large system these savings would be significant.

Two-stage and four-stage control strategies were examined. Since the four-stage control does not show significant improvement, the two-stage control seems to be sufficient as it is simple to implement and could be cost effective.

The performance of the two-stage control under cold weather condition including the internal heat generated by the occupancy related activities and solar radiation has been studied. The simulation results show that the two-stage control scheme is responsive to changes in outdoor disturbances and internal heat gains. Being simple and robust, it is a good candidate control for RFH systems.

CHAPTER 5

AUGMENTED CONSTANT GAIN CONTROL (ACGC) AND VARIABLE GAIN CONTROL (VGC)

5. 1. Introduction

The use of microprocessor based controls in residential heating and cooling applications is still not cost effective. However, this could change with the cost of microprocessor chips continues to fall and the user interface technologies continue to improve. Given this trend, it is important to develop simple control algorithm, which can be implemented with ease. With this as the motivation, in this chapter, a relative simple version of control algorithm, which can be implemented in both constant and variable gain structure is explored. The proposed algorithm will be described and simulation results will be presented to show its operating performance.

5.2. Augmented Constant Gain Control (ACGC) Algorithm

The typical modulating controller used in HVAC system is a proportional type controller. In a close-loop system, a sensor provides a feedback signal (Figure 5.2.1) of a controlled variable. This variable is compared with a setpoint and the difference, known as an error, is multiplied by a constant called the gain to obtain an output. The output signal is sent to actuator thus initiating the regulation of the process.

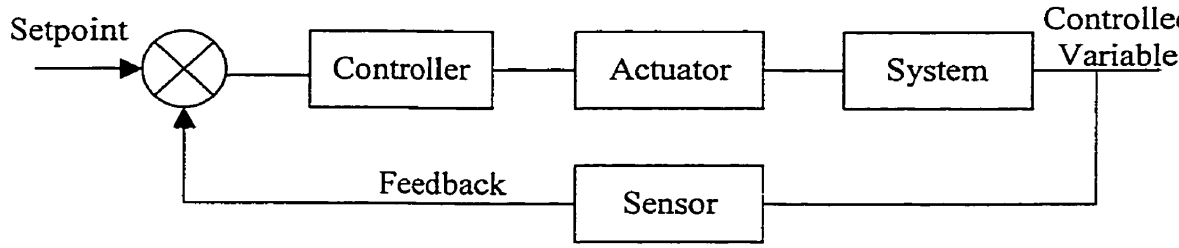

Figure 5.2.1 A close loop control system

The higher the gain the faster will be the response of the control system. However, a higher gain will cause overshoot of the controlled variable and the system could cycle infinitely. In order to improve the system stability and avoid the system responding sluggishly, an initial offset value is added such that a typical proportional controller is expressed mathematically as:

$$U = C + G \times E \tag{5.2.1}$$

There the C is the offset, G is the proportional gain and E is the error given by $E=(T_{set}-T)$.

There are several ways by which a controller can be augmented. Here a simple version is selected that can be described by the control algorithm.

$$U(n) = P \times U(n-1) + (1-P) \times K \times E(n) \tag{5.2.2}$$

Note that in Equation 5.2.2 n denotes the sampling interval. The advantage of this augmented controller is that it enables the offset term (C in Equation 5.2.1) modified to include a time varying offset which is scaled by a parameter P. The last term in Equation 5.2.2 also enhances the control algorithm through another scaling factor (1-P). The important factor in the use of this control algorithm is the design and selection of the

parameters P and K. Here a heuristic approach will be used to select the tuning parameters P and K.

5. 3. Guidelines for Selecting the Tuning Parameters

The guidelines presented in this section are as a result of several simulation runs made with the proposed control algorithm (Equation 5.2.2) on the output responses of the RFH system.

The selection of parameters P and K are based on the dynamic characteristics of the RFH system. Since the control signal U(n) in Equation 5.2.2 consists of contributions from two terms: P×U(n-1) the first and (1-P) ×K×E(n) the second, and since both terms are time varying it is instructive to consider the first one as a quasi-steady state and the second terms a dynamic term. This allows us to prescribe two different time scales to these terms. In other words, the parameter P is the weighting factor, which should reflect the overall dynamics of the RFH system segmented into two parts: steady state and dynamic. Several simulation runs carried out have shown that the dynamics of the RFH system can be easily manipulated through a control signal consisting of 70-80% of a slowly varying (steady state) signal and 20-30% of the control signal changing at a rapid rate (the dynamic part) as a function of the instantaneous error E(n).

The tuning of the gain K is somewhat difficult. In the following, simulation results are presented to show the impact of the gain on the system performance. Using these results as the basis, near optimal values of the gain are recommended.

Another potential advantage of the control algorithm (Equation 5.2.2) is that it can be used to explore a simple variable gain strategy by which the controller gain K can be updated. Such a strategy will be discussed in section 5.8. Thus the control algorithm (Equation 5.2.2) can be implemented both in constant gain control (ACGC) and variable gain control (VGC) modes.

5. 4. Comparison between Proportional Control and ACGC

Figure 5.4.1 shows the zone air temperature (setpoint 21°C) response obtained using the proportional control (Equation 5.2.1) and ACGC (Equation 5.2.2). The weighting factor P used in the simulation was 80%, and the gain factor (K) was 1.0. The proportional controller gain (G) and offset constant (C) were selected among the ones that gave good result. The figure shows that the ACGC offers faster response and smaller control value variation in zone air temperature throughout the day.

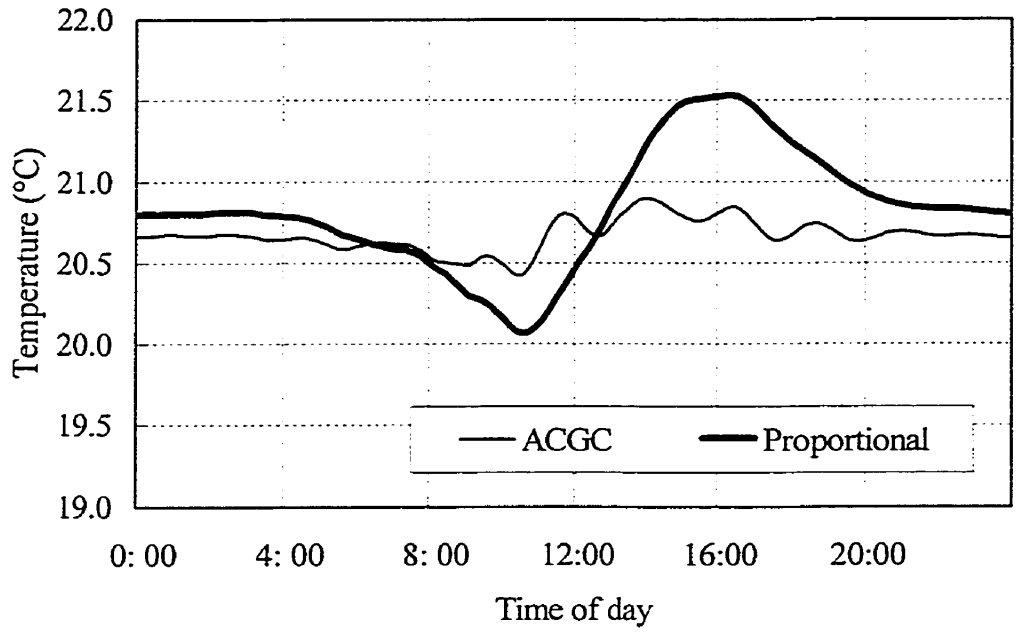

Figure 5.4.1 Zone temperature responses of proportional and ACGC

5. 5. Near-Optimal Gain Values for RFH System

Initial trial runs with the ACGC revealed that an increase in the value of P and a decrease in the gain factor K could give smooth temperature response but slow down the system response. Therefore there is a trade-off in choosing P and K. Since K is a function of dynamic variations, simulation runs were conducted to extract a functional relationship between K and outdoor air temperature for a constant P.

The step function response of the RFH system was simulated with several different values of gain factor. The outdoor temperatures were represented by a step function with magnitudes of –15°C, –10°C, –5°C, 0°C, 5°C. One set of results is depicted

in Figure 5.5.1 through 5.5.3. Starting with an arbitrary initial condition of 17.5°C, the zone temperature increases and reaches close to the setpoint (21°C). The ACGC also gives rise to steady state error, which is 0.5°C in Figure 5.5.1. As the gain factor is increased the steady state error decreases but the overshoot increases as the system response becomes faster giving raise oscillations which are dissipated as the system reaches steady state. Therefore, it is apparent that there is a trade-off between fast response time and the steady state error. A functional relationship between the gain, the steady-state error and the corresponding response time (or the number of oscillations) at various outdoor air temperatures is plotted in Figure 5.5.4. The optimum range of gain values is in between 0.9/°C to 1.1/°C for the RFH system described in this thesis.

It can also be noted from the results shown in Figure 5.5.4 that the impact of outdoor air temperature is not very significant in that a 20°C drop only induces about two oscillatory cycles.

Normally a control system has to limit the magnitude and the number of oscillatory cycles to keep the system from instability. The results of the simulations show that the best number of harmonic cycles is between 2 to 5. Form the figure we can see the best gain factor is in between of 1.0/°C to 1.1/°C. The results also suggest that as the outdoor temperature decreases, a higher gain factor will produce better system response.

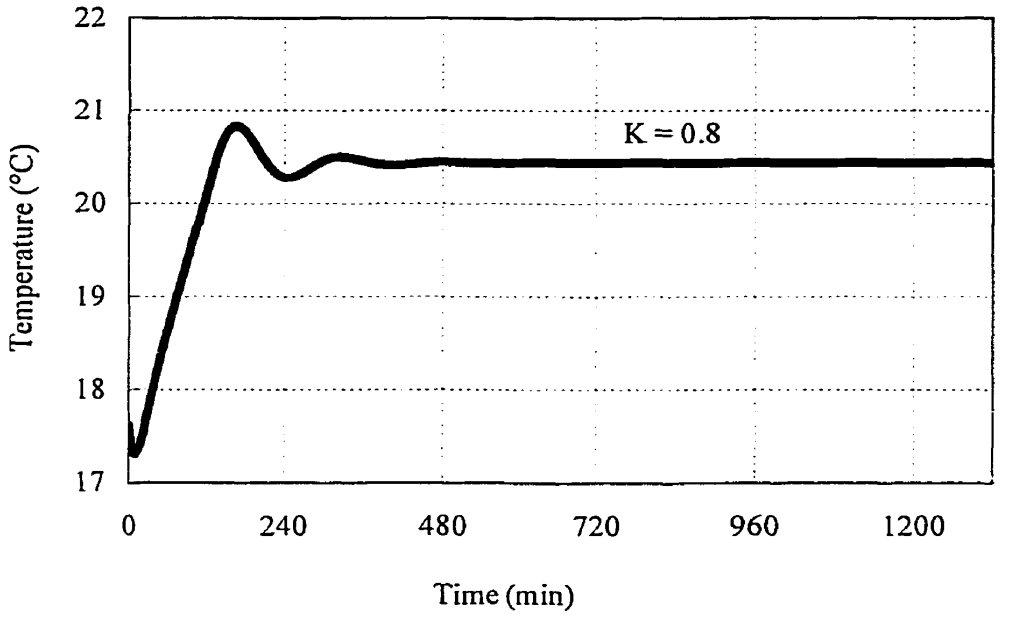

Figure 5.5.1 Temperature response to an outdoor step input –5°C, gain 0.8

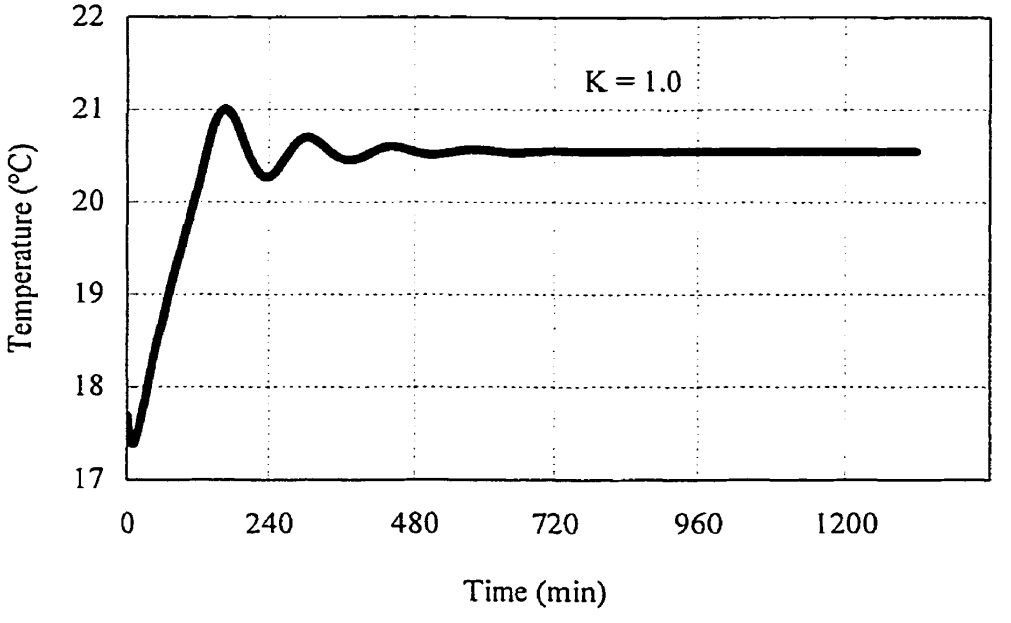

Figure 5.5.2 Temperature response to an outdoor step input –5°C, gain 1.0

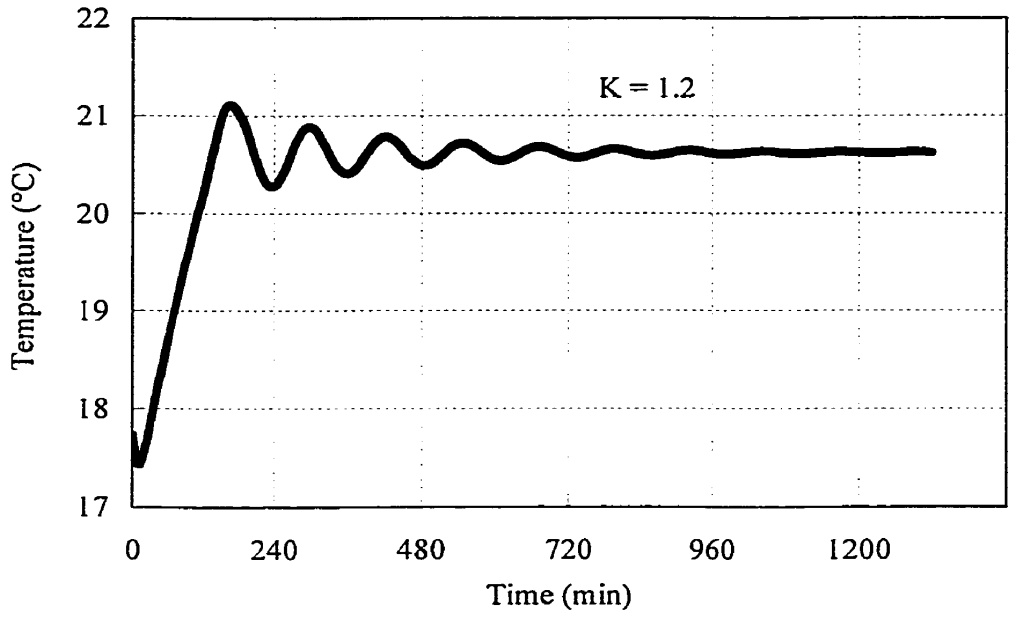

Figure 5.5.3 Temperature response to an outdoor step input –5°C, gain 1.2

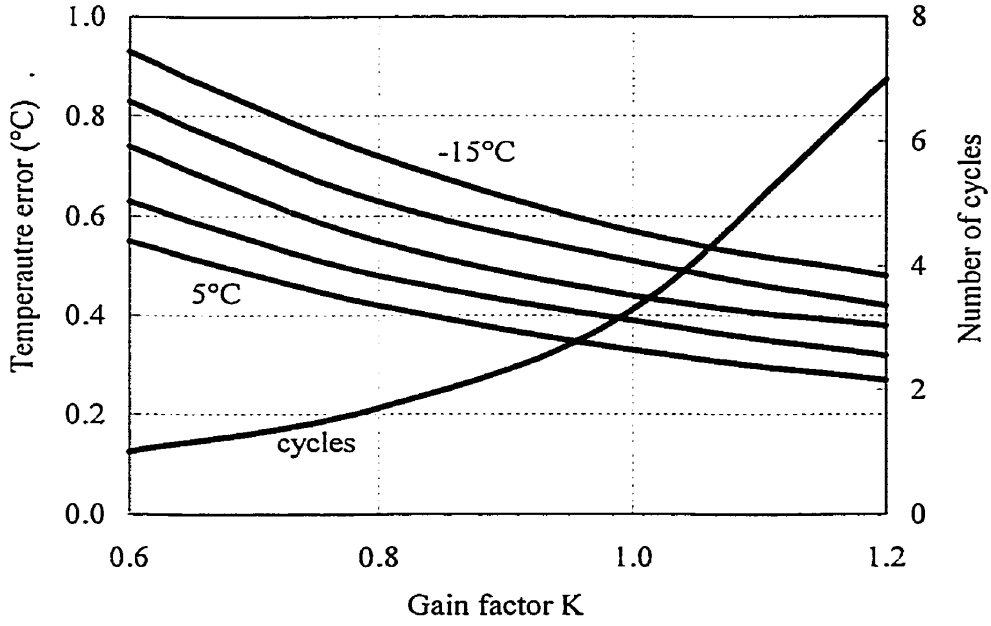

Figure 5.5.4 Near optimal gain values

The Figure 5.5.5 shows a typical daily simulation result using the optimal value of gain factor. It is apparent that zone temperature remains very nearly constant throughout the day thus showing the usefulness of the augmented control in regulating the zone temperatures in RFH systems.

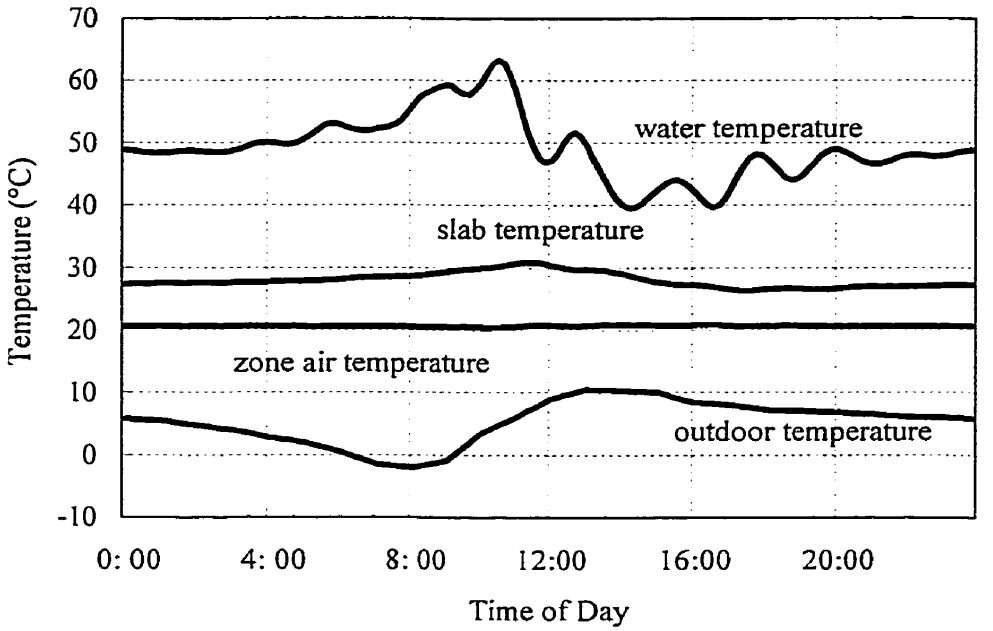

Figure 5.5.5 Typical daily responses using optimal K

5. 6. Determination of Gain for Light and Medium Structures

Most RFH system installations fall into the category of heavy structure. The simulation results presented thus for used the design data of the test facility [8] which can

also be classified as a thermally heavy structure. To examine the effect of thermal capacity of the structure on the controller gain, simulation tests were conducted for light and medium structures. The near-optimal values of gain factor obtained from the simulation runs are plotted in Figure 5.6.1, the light, medium and heavy structural classification used in this study corresponds to the ASHRAE [1] designation of thermal capacity of building enclosures. For example, a typical light structure consists of 20mm plaster, 125mm insulation and 25mm stucco and a medium structure comprises of 100mm concrete, 50mm insulation and finishing. The heavy structure details are shown in Figure 3.2.2.

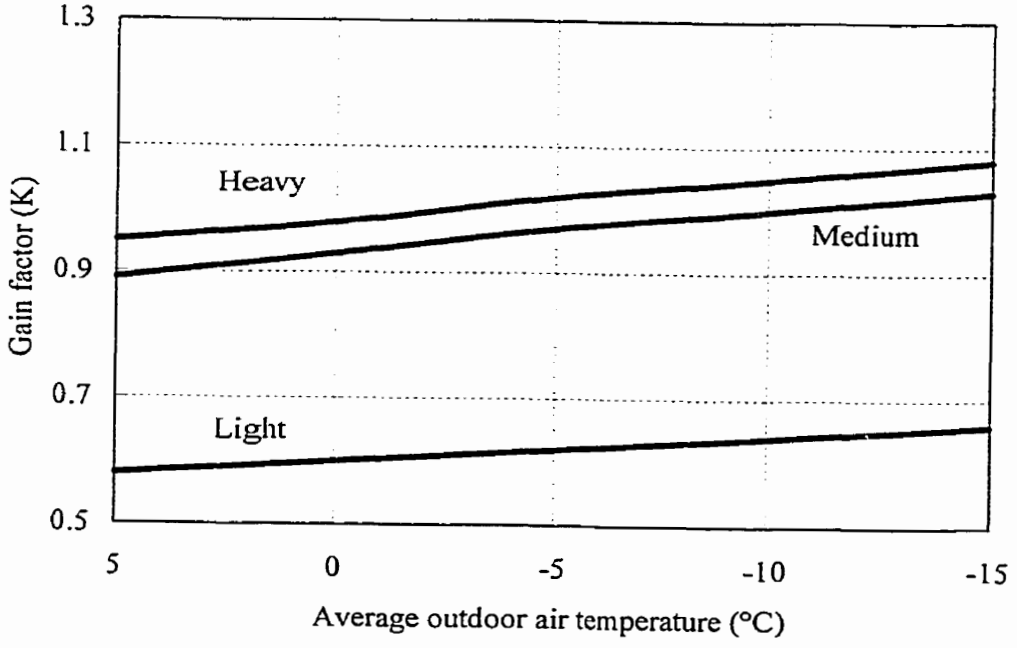

Figure 5.6.1 Near-optimal gains for light, medium and heavy structures

5.7. Decreasing the Steady State Error of ACGC

The simulation results presented in previous sections show that the ACGC gives rise to a finite steady state error which decreases as the gain factor is increased. Rather than increasing the gain, the ACGC algorithm could be modified to include a small position constant ε such that the overall response is improved and steady state error is minimized. To this end Equation 5.2.2 can be modified viz.

$$U(n) = P \times U(n-1) + (1 - P) \times K \times (E(n) + \varepsilon) \qquad (5.7.1)$$

Figure 5.7.1 and 5.7.2 show the zone temperature (setpoint 21°C) response obtained with and without ε in the ACGC algorithm. Note that, the steady state error has been reduced specially for the colder outdoor condition. Also shown in Figure 5.7.2 are the typical daily zone temperature responses. Again the advantage of including ε in the ACGC algorithm is obvious as shown by the results in Figure 5.7.2 in that the zone air temperature is closed to the setpoint with ε than without ε.

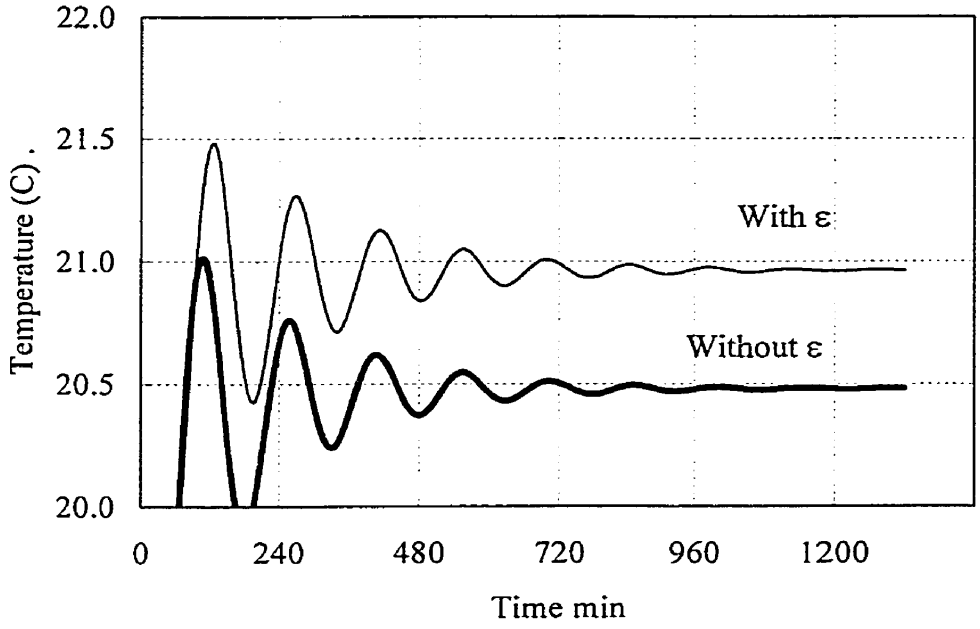

Figure 5.7.1 Zone temperature responses with and without ε for a step change in outdoor temperature

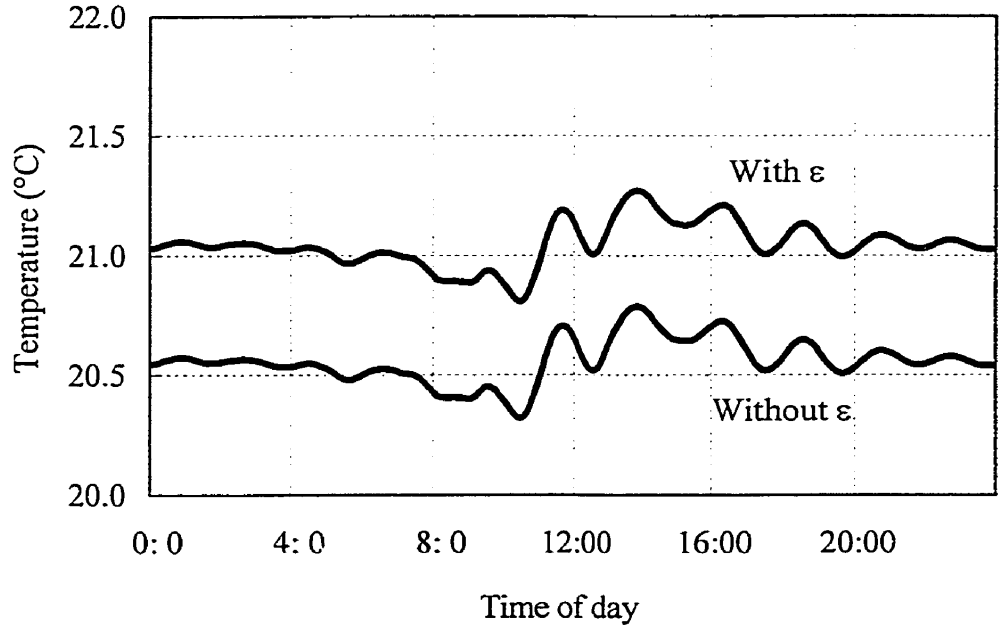

Figure 5.7.2 Typical daily zone temperature response with and without ε

5. 8. Variable Gain Controller (VGC) for RFH systems

The ACGC can be tuned using the guidelines presented in section 5.3. However, it may be possible that the controller gains so chosen may not be suitable under all operating conditions. In such an event, the gain may not be appropriate causing either oscillatory response or the excessive overshoot following a significant change in the operating conditions. To deal with this type of situations it is necessary to continuously update the gains. In other words a variable gain controller (VGC) is ideally suited in such applications.

Variable gain controller (also referred to as adaptive controllers) can be designed using available methods. However, their implementation requires significant hardware/software capabilities. For these reasons a simpler strategy will be explored by which the controller gain can be continuously updated as a function of RFH system dynamics. Such a controller is referred to here in this thesis as a Variable Gain Controller (VGC).

The controller gain factor K is a function of the overall dynamic characteristics of the RFH system which can be represented by some function viz.

$$K = f(UA,\ Ceff,\ Ta,\ Tz,\ As,\ Qin) \qquad \text{or}$$

$$K = f(q_r,\ q_c,\ qst,\ q_{int},\ U_b U_{max}) \qquad (5.8.1)$$

In order to compute the terms in RFH of Equation 5.8.1 a predictive model such as the one developed in this thesis will be required.

A simple function to define was selected, viz.

$$K(n) = \frac{[q_r(n) + q_c(n)]}{[U_b(n) U_{max} \eta(n)]} \qquad (5.8.2)$$

In other words, the VGC is a model based controller whose gains K(n) can be update using the predictions form the model. Therefore, it is important to validate and calibrate the model to achieve good control.

Figure 5.8.1 shows zone air temperature responses obtained by an optimal ACGC and VGC algorithms. It is interesting to note that the VGC performance is close to the optimal ACGC without the need for tuning. The regulation properties of VGC are stable and bounded by the model predictions.

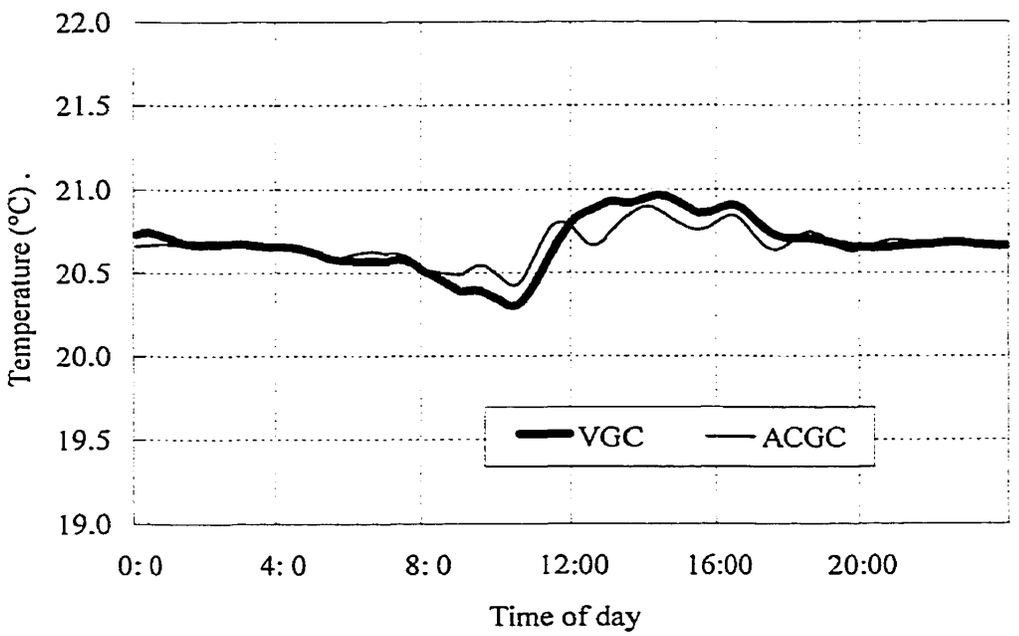

Figure 5.8.1 Zone air temperature responses of VGC and ACGC

5. 9. Summary

An augmented constant gain (ACGC) and a variable gain control (VGC) algorithms for RFH systems have been developed. The ACGC provides better performance compared to a proportion control. The stability and response time of ACGC are impacted by not only the gain but also the parameter P.

Simulation results showed that the optimal value of P for good control is 0.8. The gain of a control system is a transient parameter. It depends on weather conditions and thermal properties of the structure. Some guidelines for selecting optimum K as a function of outdoor temperature, and thermal capacity of the structure have been proposed. As the gain is increased the steady state error decreases but overshoot increases. The optimum value of gain K was found to be in between 0.9 to 1.1.

Finally, a VGC as a mean of avoiding the time consuming tuning method is proposed. The variable gain can be computed using the developed model presented in this thesis.

CHAPTER 6

CONCLUSIONS

The contributions of this thesis and conclusions that can be drawn from the research results are in the area of model development, model validation and development of improved control strategies for RFH systems. These are summarized in the following.

(i) A simple and relatively accurate dynamic model of an RFH system which includes the interactions between different subsystems (a boiler, distribution system, floor slab and building enclosure) has been developed.

(ii) By using the logarithmic-mean-temperature-difference approach, a significant reduction in the number of dynamic equations needed to model the RFH systems has been achieved.

(iii) Experimental results [8] were used to validate the model predictions. The results show that

a) The predictions from the model are in general agreement with the experimental data.

b) The thermal capacity of the floor slab was found to be an important parameter in calibrating the model with respect to measured data.

c) Model predictions were compared under several operating and control conditions. The differences between predicted and measured data were found to be $\pm 1^{\circ}C$ in the zone air temperature and $\pm 2^{\circ}C$ in the slab temperature responses.

(iv) Three control strategies for improving the temperature regulation of RFH systems are proposed.

I) A multistage control

II) An augmented constant gain control (ACGC)

III) A variable gain control (VGC)

I) Multistage control

1. By staging the control action in multiple steps, it has been shown that the temperature regulation of RFH systems can be significantly improved compared to the existing on-off controls.
2. The multistage control eliminates the use of outdoor air sensor to improve temperature control as proposed in earlier studies [24].
3. Temperature modulation was found to be more effective than mass flow modulation in terms of achieving faster response.

II) Augmented constant gain control (ACGC)

1. The ACGC tracks the zone temperature setpoint much more closely than proportional control.
2. Guidelines for selecting the tuning parameters P and K have been developed. Good temperature control was achieved with P=0.8 and K between 0.5 to 1.2.
3. Results show that as the outdoor temperature decreases and as the thermal capacity of the building enclosure is increased, a higher gain (K) value gives better control performance.

III) Variable gain control (VGC)

1. It has been shown that, the need of tuning of ACGC can be avoided by using model based control approach.
2. The variable gain was defined in terms of input and out heat fluxes. Simulation results show that the VGC is able to maintain zone temperature close to the setpoint as well as an optimal constant gain controller.

Future Research

1. Developing an analytical methodology for verifying the stability of VGC should be explored and tested.
2. Implementation and testing of multistage control, ACGC and VGC on a RFH system in a test facility should be conducted to develop implementable, cost effective controls for RFH systems.

REFERENCES

1. *ASHRAE Handbook Fundamentals*, ASHRAE, 1997;
2. *ASHRAE Handbook HVAC Systems and Equipment*, ASHRAE, 2000;
3. Athienitis, A.K., *Numerical Model of Floor Heating System*, ASHRAE Transactions 1994 part 1, pp 1024-1030;
4. Athienitis, A.K., Shou, J.G., *Control of Radiant Heating Based on the Operative Temperature*, ASHRAE Transactions 1991 part 2, pp 787-794;
5. Banhidi, L.R., *Radiant Heating systems Design and applications*, Pergamon Press, 1991;
6. Barakat, S.A, Sander, D.M., *The Utilization of Internal Heat Gains*, ASHRAE Transactions 1986 part 1, pp 103-115;
7. Brickman, R.A, Moujaes, S.F., *Numerical Modeling of Heat Transfer in A Residential Room Space Configured with Reflective Insulation and Coatings*, ASHRAE Transactions 1996 part 2, pp 32-42;
8. Cho, S, Zaheer-Uddin, M., *Temperature Regulation of Radiant Floor Heating Systems Using Two-Parameter On-off Control: An Experimental Study*, ASHRAE Transactions 1997 part 1, pp 966-980;
9. Chapman, K.S., *Thermal Comfort Analysis Using BCAP for Retrofitting a Radiantly Heated Residence*, ASHRAE Transactions 1997 part 1, pp 959-965;
10. Chapman, K.S, Zhang, P., *Energy Transfer Simulation for Radiantly Heated and Cooled Enclosures*, ASHRAE Transactions 1996 part 1, pp 76-85;

11. Chen, Q., Peng, X., Paassen, A., *Prediction of Room thermal Response by CFD Technique with Conjugate Heat Transfer and Radiation Models*, ASHRAE Transactions 1996 part 2, pp 50-60;

12. Dunne, C., Reilly, S., Ward, G., Winkelmann, F., *Algorithms for Modelling Secondary Solar Heat Gain*, ASHRAE Transactions 1996 part 2, pp 43-49;

13. Freestone, M. D., Worek, W. M., *Radiant Panel Perimeter Heating Options: Effectiveness and Thermal Comfort*, ASHRAE Transactions 1996 part 1, pp 667-675;

14. Gibbs, P.R., *Control of Multizone Hydronic Radiant Floor Heating System*, ASHRAE Transactions 1994 part 1, pp 1003-1010;

15. Hanibuchi, H., Hokoi, S., *Basic Study of Radiative and Convective Heat Exchange in a Room with Floor Heating*, ASHRAE Transactions 1998 part 2, pp 1089-1105;

16. Hogan, R.E., Blackwell, B.F., *Comparison of Numerical Model with ASHRAE Design Procedure for Warm water Concrete Floor Heating Panels*, ASHRAE Transactions 1986 part 1B, pp 589-602;

17. Kalisperis, L.N, Steinman, M, et. al, *Automated Design of Radiant Heating System Base on MRT*, ASHRAE Transactions 1990 part 1, pp 1288-1295;

18. Kilkis, B., Spapci, M., *Computer-Aided Design of Radiant Subfloor Heating Systems*, ASHRAE Transactions 1995 part 1, pp 1288-1295;

19. Kilkis, B., Coley, M., *Development of a Complete Design Software for Hydronic Floor Heating of Buildings*, ASHRAE Transactions 1995 part 1, pp 1214-1220;

20. Leigh, S.B., *An Experimental Study of the Control of Radiant Floor Heating System: Proportional Flux Modulation vs. Outdoor Reset Control with Indoor temperatures Offset*, ASHRAE Transactions 1991 part 2, pp 787-784;

21. Lindstrom, P.C., Fisher, D.E., Pedersen, C. O., *Impact of Surface Characteristics on Radiant Panel Output*, ASHRAE Transactions 1998 part 2, pp 1079-1089;

22. Ling, M., Deffenbangh, J.M., *Design Strategies for Low-Temperature Radiant Heating Systems Based on Thermal Comfort Criteria*, ASHRAE Transactions 1990 part 1, pp 1296-1305;

23. MacCluer, C.R., *The Response of Radiant Heating System Controlled by Outdoor Reset with Feedback*, ASHRAE Transactions 1991 part 2, pp 795-799;

24. MacCluer, C.R., *Analysis and Simulation of Outdoor Reset Control of Radiant Slab Heating System*, ASHRAE Transactions 1990 part 1, pp 1010-1014;

25. MacCluer, C.R., *Temperature Variations of Flux-Modulated Radiant Slab System*, ASHRAE Transactions 1989 part 1, pp 1010-1014;

26. Olesen, B.W., *Comparative Experimental Study of Performance of Radiant Floor-Heating System and A Wall Panel Heating System Under Dynamic Condition*, ASHRAE Transactions 1994 part 1, pp 1011-1023;

27. Ritter, T.L., Kilkis, B., *An Analytical Model for the Design of In-Slab Electric Heating Panel*, ASHRAE Transactions 1998 part 2, pp 1112-1114;

28. Saunders, J.H., Andrews, J.W., *The Effect of Wall Reflectivity on the Thermal Performance of Radiant Heating Panels*, ASHRAE Transactions 1987 part 1, pp 1217-1225;

29. Savery, C.W., Lee, J.B., *A Simulation Model of Electrically Heated Residences Validated with Field Data*, ASHRAE Transactions 1996 part 2, pp 3-11;

30. Scheatzle, D.G., *A Proposed Combination Radiant/Convective System for an Arizona Residence*, ASHRAE Transactions 1996 part 1, pp 676-684;

31. Simmonds, P., *Practical Applications of Radiant heating and Cooling to Maintain Comfort Conditions*, ASHRAE Transactions 1996 part 1, pp 659-666;

32. Strand, R.K., Pedersen, C.O., *Implementation of a Radiant Heating and Cooling Model into an Integrated Building Energy Analysis Program*, ASHRAE Transactions 1997 part 1, pp 949-958;

33. Watson, R. D, Chanpman, K. S., DeGreef, J. M., *Case Study: Seven-System Analysis of Thermal Comfort and Energy Use for a Fast-Acting Radiant Heating System*, ASHRAE Transactions 1998 part 2, pp 1106-1111;

34. Yost, P. A, Barbour, C. E., Watson, R. D., *An Evaluation of Thermal Comfort and Energy Consumption for a Surface-Mounted Ceiling Radiant Panel Heating System*, ASHRAE Transactions 1995 part 1, pp 1221-1235;

35. Zaheer-Uddin, M., Zheng, G.R., Cho, Sung-Hwan, *Optimal Operation of an Embedded-Piping Floor Heating System with Control Input Constrains*, Energy Conversation Management, Vol. 38. No. 7, 1994, pp 713-725;

36. Zhang, Z., Pate, M.B., *An Experimental Study of the Transient Response of a Radiant Panel Ceiling and Enclosure*, ASHRAE Transactions 1986 part 2, pp 85-94;

37. Zhang, Z., Pate, M.B., *A numerical Study of Heat Transfer in a Hydronic Radiant Ceiling Panel*, ASME 1986 HTD-val. 62, pp 31-38;

APPENDIX

C++ PROGRAM

1. Objects Declaration

```
//----------------------------------RFH.H---------------------------------
/* This program is written for objects declaration including:
boiler, floor, room, and controllers.
*/
//boiler declaration:
class boiler
{
        double Ub;                      //fuel supply from 0 to 1
        double Uw;                      //water mass from 0 to 1
        double Tin;                     //entering water temperature

public:
        static double Tout;             //water off temperature
        boiler(double water, double Ti, double f);
};

//radiant floor slab declaration:
class flor
```

```
{
        double Uw;                  //water mass flow
        double Tsp, heat;           // supply water T and floor release H
        static double T1, T2;
        double dTrt, dTslab, dT1, dT2;
public:
        static double Trt;
        static double Tslab;
        flor(double wt, double Ts, double Q);
};

//room enclosure declaration:
class room
{
        double Tslab, Toutair, solar;
        double dTiwall, dT1, dT1, dTowall;
        static double T1, T2;
public:
        static double Tair;         //zone air temperature
        static double Tiwall, Towall; //interior and exterior temperature
        room(double Tsl, double To, double Sl);
};
//on-off controller:
```

```
class onoff
{
        double Hlimit;          //high limit
        double Llimit;          //low limit
        double reference;       //control variable
public:
        double controlval;
        onoff(double h, double l, double r, double c);
};

//two-stage on-off controller:
class twostage
{
        double reference;
public:
        double controlval;
        twostage(double ref, double val);
};
```

2. Definitions of Declarations

```
//-----RFH.cpp-----------
```

```
#include <math.h>
#include "RFH.H"
//thermal capacitance
#define Cpw 4186.8          //specific heat of water in J/kgK
#define Cp 1.9e06           // thermal capacitance of floor panel in J/K
#define Cb 4.24e04          // thermal capacitance of boiler in J/K
#define Cz 4.2e06           // thermal capacitance of zone in J/K
//boiler parameters
#define alpha 0.12          //constant for calculating efficiency
#define ab 5.06072          //rate of boiler jacket heat transfer W/K
#define Ubmax 7500          //boiler capacity in W
#define Tbmax 62.0          //high temperature limit of water in C
#define Te 20.0             //boiler room air temperature in C
//return water
#define Uwmax 5/60          //max water mass flow in 5L/min
#define Up 13.5             //13.5
//zone data
//#define az 110            //zone U-value in W/K
//panel data
#define Mw 7.55             //water mass inside of tube in kg
#define hit 140.2           //water side convection coefficient of tube
W/K
#define Ait 12.36           //inside tube area m2
```

```
#define Ap 13.2                    //floor slab surface area m2
#define dt 1                       //time step in sec

double Air_Temp(double, double, double, double, double);

//boiler object definition, inputs include water flow, water temperature and fuel
double boiler::Tout=60;
boiler::boiler(double w, double ti, double f)
{
        Uw = w;                    //water flow rate from 0 to 1
        Tin = ti;                  //entering water temperature C
        Ub = f;                    //fuel input from 0 to 1
        Tout += (Ub*Ubmax*(1-alpha*Tin/Tbmax)-
                Uw*Uwmax*Cpw*(Tout-Tin)-ab*(Tout-Te))*dt/Cb;
}

//heating floor slab definition,
//input include water flow, entering temperature and heat release
double flor::Trt=50;               //water off temperature C
double flor::T2=35;                //middle of the slab C
double flor::T1=30;                //bottom of the slab C
double flor::Tslab=30;             //surface of the slab C
```

```
flor::flor(double wt, double Ts, double q)
{
        Uw = wt;                //water flow form 0 to 1
        Tsp = Ts;               //entering water temperature C
        heat = q;               //heat release of last step W

        double lmtd             //log mean temperature difference
        if (Uw==0) lmtd=0;
        else lmtd=( Tsp- Trt)/log((Tsp- T2)/( Trt- T2));

        dTrt=(hit*Ait)*dt/(Mw*Cpw)*(lmtd)+ Uw*Uwmax*dt/Mw*(Tsp-Trt);

        dT2=(2*Uw*Uwmax*Cpw*(Tsp-Trt)+heat*Ap
                -3*Up*Ap*(2*T2-Tslab-T1))*dt/Cp;

        dTslab=((-Ap*heat-Up*Ap*(Tslab-T2))*dt/(Cp/6)-dT2)/2;

        dT1=((Up*Ap*(T2-T1))*dt/(Cp/6)-dT2)/2;

        Trt += dTrt;
        T1 += dT1;
        T2 += dT2;
```

```
        Tslab += dTslab;
}

//zone definition, inputs include surface temperature of floor slab
//outdoor air temperature and solar radiation
double room::Tair=20;                   //zone air temp
double room::Tiwall=15;                 //inside surface
double room::T1=12;
double room::T1=8;
double room::Towall=7;                  //outside surface

room::room(double ts, double to, double sl)
{
        Tslab = ts;             //heating floor slab surface temperature C
        Toutair = to;           //outdoor air temperature C
        solar = sl;             //solar radiation intensity W/m2

        double qr=5*(pow(((Tslab+273)/100),4)
                        -pow(((Tiwall+273)/100),4));
        double qc=1.31*pow((Tair-Tiwall),1.33);

        dT1 = (-(qr*Ap+44.8*qc+2.25*0.9*solar) -3*350*(T1-Tiwall)*
                        -2*25.8*(T1-T2))*dt/(Cz/3);
```

```
        dT2 = ((-44.8*(solar-34*(Towall-Toutair))
                        -3*az*(T2-T1)-2*az(T2l-Towall))*dt
                        /(Cz/6);

        dTiwall=((2*(qr*Ap+44.8*qc+2.25*0.9*solar)
                        -3*350*(Tiwall-T1) +2*25.8*(T1-T2))*dt
                        /(Cz/3);

        dTowall=((44.8*(solar-34*(Towall-Toutair))
                        -3*730*(Towall-T2)+25.8*(T2-T1))*dt
                        /(Cz/6);

        Tiwall += dTiwall;
        T1 += dT1;
        T2 += dT2;
        Towall += dTowall;

        Tair = Air_Temp(44.8,Tiwall,Ap,Tslab,Toutair);
}

onoff::onoff(double h, double l, double r, double c)
{
        Hlimit = h;
```

```
        Llimit = l;
        reference = r;
        controlval = c;

        if (r <= Llimit) controlval = 1.0;
        else if (r >= Hlimit) controlval = 0.0;
}

twostage::twostage(double ref, double val)
//two-stage control air temperature setting 21C
{
        reference = ref;
        controlval = val;

        if (reference>=22.0) controlval=0.0;
        if (reference>20.5 && reference<21.5)
                controlval=0.5;
        if (reference<=20.0) controlval=1.0;
}
```

3. Functions

```
//--------Air_Temp.cpp---------------------------
```

```
//this function is written for computing zone air temperature


#include <math.h>
double Air_Temp (    double AE,          //area of enclosure
                     double TE,          //temperature of enclosure interior surface
                     double AF,          //area of floor
                     double TF,          //temperature of floor surface
                     double TOUT)        //outdoor temperature
{
        double high, low;
        double A, B;
        double ta, infiltration;         //ta is zone air temperature

        high = TF;                       //initial selection of high boundary of ta
        low = TE;                        //initial selection of low boundary of ta
        ta = (high+low)/2.0;             //initial selection of ta
        infiltration = 0.5*AF*3.8/3600*(ta - TOUT);        //infiltration ACH is 0.5

        A = 2.31*AF*pow((TF-ta), 1.31);          //convection heat transfer in floor
        B = 1.31*AE*pow((ta-TE), 1.33)           //convection heat transfer in wall
                + infiltration;
        do
        {
```

```
            if (A<B) high = ta;     //update of high boundary of ta
            else low = ta;          //update of low boundary of ta
            ta = (high+low)/2.0;    //update ta
            A = 2.31*AF*pow((TF-ta), 1.31);
            B = 1.31*AE*pow((ta-TE), 1.33)+ infiltration;
            infiltration = 0.5*AF*3.8/3600*(ta - TOUT);
        }
        while (fabs(A-B) < 0.00001);
        return ta;
}
```

4. Main Program

```
//-------VGC.cpp---------
// This is written for simulating the ACGC and VGC system.
#include <stdio.h>
#include <stdlib.h>
#include <math.h>
#include "RFH.H"

#define totaltime 2             //compute time in days

double Toutdoor(int);
```

```
double Solar(int);
void main()
{
        double qc, qr;
        double To, Sol;
//initial settings
        double fel = 0.4;
        double wtr = 1.0;

        double Tbsp=55.0;    //boiler water off temperature C
        double Tbrt=43.0;    //boiler water entering temperature C
        double Twsp =55;     //water supply temperature to slab C
        double Twrt =48;     //water return temperature from slab C
        double Tws = 43;     //inside slab temperature C
        double Tsl = 30;     //slab surface temperature C
        double Twl = 19;     //wall interior surface temperature C
        double Two = 0;      //wall exterior surface temperature C
        double Ta = 21;      //zone air temperature C

//boiler variable energy input control
        double percent = 0.9;
        double K=1.1;
        double Ein=0.0, Eout=0.0;
```

```
        int day, hour, sec, dt;


//write output to text file named test.dat
        FILE* fp;
        if ((fp=fopen("data.dat","wt"))==NULL)
                printf( "The file data.dat was not opened\n" );
        else
        {
                fprintf(fp,"%s\t%s\t%s\t%s\t%s\t\n",
                "Time", "Return Water", "Floor Slab", "Zone Air", "Outdoor Air");


                for (day = 0; day < totaltime; day++)
                for (hour = 0; hour < 24; hour++)
                for (sec = 0; sec < 3600; sec++)
//              for (dt = 0; dt < 600; dt++)    //time step in 1/600 sec
                {
                        int t = hour*3600+sec;
                        To = Toutdoor(t);
                        Sol = Solar(t);         //solar radiation intensity
//output last day's data in min
                        if ((sec%600==0)&&day == (totaltime-1))
                        {
//                              hour = hour+16;         //start at 16:00
```

```
//                      if (hour >= 24) hour = hour-24;

        fprintf(fp,"%2d:%2d\t%8.3f\t%8.3f\t%8.3f\t%8.3f\\n",
                                hour, sec/60, Twsp, Tsl,  Ta, To);
                    };
                    qr=5*(pow(((Tsl+273)/100),4)-pow(((Twl+273)/100),4));
                    qc=2.18*pow(fabs(Tsl-Ta),1.13);

                    if (day == (totaltime-1))
                    {
                        Eout = 4.4*3*(qr + qc);
                        Ein = (7500*fel*0.88);          //efficiency 88%
                        K = Eout/Ein;
                    };
                    fel = percent*fel + (1-percent)*K*(21-Ta);
                    if (fel <= 0) fel =0.0001;        //minimum input
                    if (fel >1) fel =1;               //maximum input

                    boiler B(wtr, Twrt, fel);
                    flor F(wtr, Twsp, (qc + qr));
                    room R(Tsl, To, Sol);

                    Twsp = B.Tout;
```

```
                Twrt = F.Trt;

                Tsl = F.Tslab;

                Ta = R.Tair;

            };

        };

}
```